Long-Range Forecasting and Climate Research

The climate of the World

III — El Niño/Southern Oscillation and the Quasi-biennial Oscillation

by

C.K. Folland and D.E. Parker

LRFC 3

March 1986

Meteorological Office (Met. O. 13)
London Road
Bracknell
Berkshire RG12 2SZ

LONG RANGE FORECASTING AND
CLIMATE RESEARCH MEMORANDUM NO. 3
(LRFC 3)

THE CLIMATE OF THE WORLD
III - EL NINO/SOUTHERN OSCILLATION AND THE QUASI-BIENNIAL OSCILLATION

by

C K FOLLAND AND D E PARKER

BASED ON AN ADVANCED LECTURE DELIVERED
TO THE SCIENTIFIC OFFICERS' COURSE,
METEOROLOGICAL OFFICE COLLEGE, MARCH 1985

Met O 13 (Synoptic Climatology Branch)
Meteorological Office
London Road
Bracknell
Berkshire RG12 2SZ

March 1986

This Memorandum is the third is a series of six on:

THE CLIMATE OF THE WORLD

BY

C K FOLLAND AND D E PARKER

Based on nine Advanced Lectures delivered by C K Folland to the Scientific Officers' Course 1-7 March 1985, and one Advanced Lecture delivered by D J Carson in March 1982.

INDEX TO SERIES

LRFC 1	INTRODUCTION AND DESCRIPTION OF WORLD CLIMATE (Advanced Lectures 1 and 2). C K Folland.
LRFC 2	FORCING AND FEEDBACK PROCESSES (Advanced Lectures 3 and 4). C K Folland.
LRFC 3	EL NINO/SOUTHERN OSCILLATION AND THE QUASI-BIENNIAL OSCILLATION. (Advanced Lecture 5). C K Folland and D E Parker.
LRFC 4	CLIMATIC CHANGE: THE ANCIENT EARTH TO THE "LITTLE ICE AGE" (Advanced Lectures 6 and 7). C K Folland.
LRFC 5	CLIMATIC CHANGE: THE INSTRUMENTAL PERIOD (Advanced Lecture 8). C K Folland and D E Parker.
LRFC 6	CARBON DIOXIDE AND CLIMATE (WITH APPENDIX ON SIMPLE CLIMATE MODELS) (Advanced Lecture 9 plus an Advanced Lecture delivered by D J Carson in March 1982). D E Parker, C K Folland and D J Carson

ADVANCED LECTURE NO 5

PART I - THE EL NINO - SOUTHERN OSCILLATION (ENSO)

5.1.1 Introduction

The term El Nino (The "Christ Child") was originally given to a weak warm coastal current which commences around Christmas and flows southwards along the coast of Ecuador and Peru during each Southern Hemisphere summer. Every few years the near-coastal warming associated with the current becomes particularly intense (4-7°C); during the following 12 months the entire Central and Eastern tropical Pacific Ocean warms typically by 1-3°C. In 1982-83, the warming in the open ocean near 130°W, 5°S, caused SST to reach almost 6°C above normal in December 1982, an amount which can usefully be compared with the annual cycle of SST for the world shown in Lecture 4, Fig 4.9

Fig 5.1 shows the observed SST in the Pacific and Fig 5.2 the observed sea surface temperature anomaly (SSTA) during the N Hemisphere winter of 1982-83 and near the most intense phase of one of these tropical Pacific warmings (Quiroz (1983)). The term 'El Nino' is now generally used by climatologists to describe the widespread ocean warming and not the local coastal warming. Fig 2.5, Lecture 2, showed mean January SST for 1951-80; it can be seen that the normal east-west gradient of tropical Pacific SST has not only nearly disappeared in Fig 5.1 but that the absolute maximum SST in the period between Dec 1982-Feb 1983 was placed about 60°E of its normal position. The 1982-83 El Nino will be discussed below; Quiroz gives a very good observational account.

High surface temperatures are only one aspect of the anomalous behaviour of the Tropical Pacific Ocean during an El Nino: the entire thermal and dynamic structure of the upper ocean is different from normal (Gill and Rasmusson (1983)) (see later). The presence of such a large anomalous heat source at the lower boundary of the tropical atmosphere can be expected to affect the atmospheric general circulation and it has become clear over the last 20 years that a near global scale PMSL sea-saw known for half a century as the Southern Oscillation (SO) is linked to El Nino.

The possible existence of a large-scale interannual PMSL fluctuation was first hinted at by a Swede, Hildebrandsson in 1897 who found an out of phase relationship between PMSL at Sydney, Australia and Buenos Aires, Argentina. Lockyer and Lockyer uncovered the worldwide scale of the PMSL fluctuation in 1902-6 but Walker and Bliss (1923-37) provided the first detailed analyses of the companion temperature and rainfall fluctuations and were the first to name the phenomenon the "Southern Oscillation". See Rasmusson and Carpenter (RC) (1982) for historical detail and references. Fig 5.3 shows the correlation between annual PMSL anomalies at Easter Island and many other stations distributed worldwide produced by Berlage and de Boer (1959), confirmed several times since Berlage and de Boer's paper. Djakarta, Java and Easter Island are 140° of longitude (15,000 km) apart and all investigations agree on a negative correlation of -0.9 or so between their annual or even seasonal mean PMSL values. Fig 5.4 shows the average January PMSL in the Pacific (1961-76) and the position of some of the "key" stations that will be used in the description. The SO fluctuations are usually monitored by an SO index (SOI) which has been

defined in many ways; Fig 5.3 indicates that the simplest and best index might be simultaneous values of (Easter Island - Djakarta) PMSL.

Returning to relationships between SO and Argentinian climate, Fig 5.5 shows superimposed time-series of the level of the great Parana river and an SO index about a century ago (correlation 0.56). However due to better data quality and availability Tahiti and Darwin PMSL have often, if less satisfactorily, been used to provide an SO index. Fig 5.6 shows the normalised pressure difference between Tahiti and Darwin updated from Parker (1983) and Fig 5.7 shows a time series of seasonal SSTA for 1856-1984 (from 1951-60 average) calculated for the Tropical E Pacific (170°E - S American coast, 20°N-20°S) an area of about 45 x 10^6 km^2, taken from Folland et al (1985). The correlation between 3 month seasonal mean Tropical E Pacific SSTA and SO indices between 1935-80 is about -0.65 ie warm SSTA is associated with a negative SO index. The tropical E Pacific SSTA variations are (in the main) part of a worldwide fluctuation of SSTA. This is most readily shown in Fig 5.8 (from Folland et al (1985)) which shows the second (correlation matrix) eigenvector (EOF2) of worldwide SSTA calculated for each season and for the available 10° x 10° areas between 1901-80. The time series of the amplitude of EOF2 is shown in Fig 5.9 together with that of the tropical E Pacific SSTA variations; the two time series of EOF2 are strongly correlated. EOF2 does not allow for systematic developments in the shape of the worldwide SSTA patterns which might occur as "ENSO events" develop or real differences in pattern between events. Despite these limitations a strong, consistent, warming of the Indian Ocean and the NE Pacific and a similar tendency for simultaneous negative SSTA in the NW Pacific when the tropical C and E Pacific are warm is apparent. (Values of the terms of EOF2 of magnitude about 40 or over (Fig 5.8) reflect a reasonably consistent relationship with tropical E Pacific SSTA). Fig 5.10 shows a spectrum of seasonal tropical E and W Pacific SSTA and marine air temperature for 1861-1980 from Folland et al (1985) and shows the time scales of variation. The E Pacific (basically El Nino variations occupy the 2.5-16 year time scales. The W Pacific spectrum is distinctly different, being much "whiter".

5.1.2 Global temperature variations associated with El Nino

5.1.2.1 SSTA

Newman (1984) has carried out a detailed analysis of the typical worldwide SSTA variations associated with the various phases of El Nino over about the last century. The years quoted below are usually the first of the consecutive years that were affected by El Nino (the first is called year (0)). The 17 El Nino events identified were: 1888, 1896, 1899, 1902, 1905, 1918, 1930, 1939, 1940, 1941, 1951, 1957, 1965, 1969, 1972, 1976 and 1979. 1982 was certainly an El Nino year but data was not available for Newman's study. 1877-78 was an El Nino year but with too few data for analysis. Composite monthly global SSTA charts are shown for April, August and December of year (0) and March of year (+1) (Fig 5.11(A)-(D)).

The early stages in the development of an El Nino during which the warming is confined to S American coastal waters is not well represented because the 5° x 5° area resolution used was too coarse. By April of year 0, the S Pacific near the western coast of South America as far south as 35°S shows a distinct warming. A tongue of positive SSTA extends westwards

from the South American coast along the Equator, reaching 130°W in May and 170°E by July. The SSTA pattern intensifies, so by September a large proportion of the Tropical Pacific is warmer than normal and by up to 2°C in the east. In December the warming is at its peak with maximum mean SSTA of 2°C to 3°C. In year (+1) SSTA decline. Both Indian and Tropical Atlantic Oceans warm during El Nino, starting in late summer of year (0). By March of year (+1) much of the Atlantic from 30°N to 30°S is warmer than normal by between .2° and .5°C. The Indian Ocean exhibits maximum mean SSTA of up to .6°C in January of year (+1).

By contrast, in April of year (0) an area in the central N Pacific, centred near 30°N, is weakly cool; then the negative SSTA spread northwards and strengthen, giving mean anomalies of -.8°C in some areas near 40°N between July and October. From November of year (0) to March of year (+1) negative SSTA persist, but are generally weaker. In the North East extratropical Pacific an area of anomalous warmth spreads northwards near the North American coast in October. This warm area persists until after March of year (+1). From October to December of year (0), the north east Atlantic, polewards of 35°N, is weakly cool with a suggestion of cool SSTA south of 40°S, common to much of the Southern Ocean. The data is too sparse to be certain, however.

RC used SSTA measured between 1953 and 1974 along 6 ship routes in the area 20°N to 20°S, 70°W to the dateline, to investigate the growth and movement of tropical Pacific SSTA during El Nino. The most common time scales of SSTA fluctuations associated with El Nino (in the area and for the period defined above) were found to be between 36 and 43 months. Cross spectral analysis of SST data at different longitudes indicated that the large scale positive SSTA which initially appear off the coast of Peru about December (eg at Puerto Chicama, see "PC" on Fig 5.4), spread westward along the Equator, reaching 170°W in 3-6 months. They also noted that SSTA appeared to modestly increase almost simultaneously near the equator at about 170°W. The average westward propagation of SSTA has a speed of of .5-1.0 m s^{-1}. RC also noted a warming of the ocean west of Chile in latitudes 30-35°S in the year (-1) preceding El Nino.

El Ninos vary considerably in character and in the time intervals between them (eg 3 years between 1969 to 1972, but nine years from 1942-51). This variability may prove crucial to our understanding. For example: the Tropical Pacific west of the dateline was markedly warmer in 1976 than 1972; in the 1982 event the Tropical E Pacific warmed before the S American coast, which warmed most at the end of the ENSO event, in April-June 1983.The Tropical E Pacific remained warm well into autumn 1983, ie year (+1), and widespread warming of the Indian Ocean exceeded 1.5°C. In 1976, the warming of the Indian Ocean area was weak. The years between 1972 and 1982, during which there were 4 El Ninos (3 of them strong), contrasts with the periods 1942-50 and 1879-1887 when there were none while between 1907 and 1938 El Ninos were few or rather weak (Fig 5.7).

5.1.2.2 Atmospheric Temperature Variations

Pan and Oort (1983) have given a zonal mean latitude-height cross section of mean temperature differences between three pairs of years having warm and cool East Pacific SST respectively (Fig 5.12) for northern winter. The troposphere as far poleward as 45°N and S warmed by up to 1°C at 400

mb, presumably due to increased moist convection in the tropics. Note also the cooling at middle and high latitudes of about -0.5°C in the Northern Hemisphere, which matches the underlying SST changes fairly well.

Pan and Oort also showed that specific humidity rose where air temperature rose and also fell slightly in high latitudes. It is interesting that a tropical forcing (warming) from below has warmed the global troposphere as a whole but that the atmospheric circulation has changed so as to provide a weak cooling in high latitudes. This is rather unexpected, perhaps.

5.1.3 Atmospheric Variations

5.1.3.1 General Description

There is now a considerable literature on aspects of the general circulation associated with ENSO or suspected to have a connection with it. The background climatology is described by Horel (1982). RC and Wyrtki (1975) have both shown that ENSO is associated with variations in the Pacific trade wind circulations and the latter author, sea level fluctuations in the Pacific. Chen (1982) and Horel and Wallace (1981) have indicated links with the Northern Hemisphere mid-latitude circulations; van Loon et al (1982) report associations with the stratospheric circulation and Angell (1981) reports associations with ozone over North America and the water vapour content of the low stratosphere; Bacastow and Keeling (1981) note a link with tropospheric CO_2 content. ENSO has been proposed as a long range forecasting tool for the Indian monsoon by Shukla and Paolino (1983) and has been used to help make long range forecasts in the USA and New Zealand. Tropical Pacific SST variations (now defined separately in the Central and East Pacific) have recently been introduced, usefully, as a factor in a statistical long range forecasting technique used in the Synoptic Climatology Branch of the Meteorological Office (Maryon and Storey, 1985). The contrast between El Nino and "La Nina" (cold east tropical Pacific) is discussed by Philander (1985).

5.1.3.2 Tropical Atmospheric Variations

The tropical atmosphere is perturbed during ENSO in a complex way as indicated by RC and other authors. In the winter and summer (S Hemisphere) preceeding El Nino, the south east trade winds between 120°W and the dateline are usually abnormally strong giving wind stresses over the tropical S Pacific 50-80% above normal. Relaxation of this stress to below normal levels in the tropical W Pacific in the next summer is followed by the start of El Nino - sometimes the wind stress is reversed ie the winds become westerly. The reason for the weakening is not known, though wind stress is usually less in summer in this region. During year (0) of El Nino, the easterly component of wind stress reaches a minimum but increases once more later in year (0). By contrast, near the equator, between 90°W and about 130°W, the E to SE trades increase in strength to reach a peak during year (0).

The spatial distribution of surface wind anomalies reflects changes in the positions of the Inter-Tropical Convergence Zone (ITCZ) and the South Pacific Convergence Zone (SPCZ) (see Lecture 2). The convergence zones are important in determining the areas of active convection and hence

areas of latent heating in the middle and upper troposphere and the rain falling on the "desert" islands of the equatorial Pacific (Lecture 2). Changes in the trade wind circulation also reflect changes in the intensity of the Indonesian Low and Easter Island High, which as described above, are often used to indicate the phase of the SO.

Figs 5.13(A)-(C) show the anomalous mean tropical Pacific surface winds in an El Nino composite study carried out by RC, shown here for August-October (-1), March-May (0) and December (0) - February (+1). In autumn of year (-1) surface wind anomalies are generally small except to the north-east of Australia where anomalous northwesterlies tend to occur and the SPCZ is displaced to the southwest of its normal position. The South Pacific High then weakens but the Indonesian Low changes little. Wind anomalies increase from November (-1) to March (0) with a strong anomalous westerly component (not always giving absolute westerlies) developing south of the Equator and north of 10°S from 170°E to 170°W, reflecting a reduction in strength of the south-east trades. The Indonesian Low fills while the Easter Island High continues to decline. From March to May (0) the same trends in the pressure field continue. Between 110°W and 170°E, ITCZ is now displaced south of its normal position with anomalous northerlies on its northern side. The anomalous westerly component just south of the Equator now reaches 160°W and there is a strengthening of the south-south east trades in the latitude band 30°S to 10°S from east of Australia to the dateline.

During the remainder of year (0) the anomalous features noted above intensify. In particular the ITCZ continues to be placed south of its climatological position and the SPCZ now becomes located markedly north east of its usual location, reducing the size of the equatorial dry zone (centred near the dateline) between them. During August-October of year (0) the equatorial westerly anomalies are at their strongest exceeding 2 ms^{-1} over much of the Tropical Pacific west of 160°W and an anomalous surface wind convergence is centred near 150°W close to the equator. The Pacific High begins to build again about July followed by a deepening of the Indonesian Low about November. As the El Nino year progresses, the surface wind convergence maximum moves eastwards to near 130°W, the westerly anomaly decreases and the south east trades strengthen between 140-180°W, ie west of the wind convergence.

Pan and Oort (1983) correlated SST in a key area near 2.5°S, 130°W (assumed to represent the entire Tropical E Pacific, a reasonable assumption in view of SSTA analyses presented in Section 5.1.2.1) with global fields of 850 mb and 200 mb wind components and 500 mb vertical velocity.

They found that warm SST (El Nino) is associated with:-

i. Anomalous ascent of air over the Central and much of the Eastern Equatorial Pacific, with anomalous descent of air east of 120°W, over the western Pacific between 110°E and 150°E, and over the subtropics.

ii. An increase in the 200 mb subtropical westerlies in both hemispheres near 25° latitude, with anomalous 200 mb easterlies over the Equatorial Pacific, roughly west of the main SSTA maximum.

iii. A weakening of surface and 200 mb westerlies near 60°N.

Pan and Oort note that these observations are consistent with Bjerknes' pioneering (1969) explanation of ENSO. Bjerknes (1969) suggested that the normal nearly east-west equatorial Pacific Walker cell, in which air ascends in the convectively active area around Indonesia and descends over the Eastern Pacific near 90°W, is weakened during El Nino. Fig 5.14 shows this cell in more detail (from Kousky et al (1984)). See Lecture 2 for "Walker" cells.

The warm tropical ocean causes the Hadley cell to intensify, leading to stronger 200 mb subtropical jets. In Section 5.1.2.1 it was noted that all three tropical oceans warm during El Ninos, which is consistent with the intensification of subtropical jets at all longitudes. A decrease in the westerlies at 60°N is seen by Pan and Oort as evidence for a stronger than normal Northern Hemisphere Ferrel cell.

Selkirk (1984) has provided an up-to-date analysis of the 200 mb flow associated with El Nino. He usefully discusses the fluctuations in the light of predictions made by linear models, eg that of Simmons (Fig 4.19) (in Lecture 4), which shows how the 200 mb and lower tropospheric winds might respond to an anomalous (here a C or E Pacific) heat source.

5.1.3.3 Extra Tropical Relationships with El Nino Events

Many authors have found that the El Nino is associated with changes in extratropical circulations, though teleconnections are less well defined than in the tropics.

Chen (1982) correlated seasonal values of the Tahiti-Darwin SOI with Northern Hemisphere 700 mb geopotential height between 1950 and 1979. He also carried out a composite analysis of the 700 mb data stratified according to SOI. The simultaneous correlations are shown in Figure (5.15). The winter pattern is quite similar to the 'Pacific North America (PNA)' teleconnection pattern found by Horel and Wallace (1981) (Fig 5.16) with three centres of response situated at 40°N, 145°W, (high positive correlation), Canada near 125°W (large negative correlation) and near Florida extending towards Spain (high positive correlation). Correlations between the height field and SOI of later seasons drop sharply and also as the lag of SOI behind the 700 mb fields increases. By contrast, correlations reach a maximum when SOI leads the 700 mb fields by one or two seasons, the response pattern staying broadly similar. However, only in winter with SOI leading the 700 mb data by one or two seasons is statistical significance at the 95% level unequivocably obtained.

Chen's composite analyses enable non-linearity in the Northern Hemisphere 700 mb atmospheric response to variations in SOI to be studied. Chen finds that 700 mb height anomalies over the Atlantic are more pronounced with high SOI (low E Pacific SST) (Fig 5.15(a), (b)).

5.1.3.4 Rainfall Variations

Equatorial rainfall anomalies are an important aspect of El Nino events because of their obvious implications for Pacific 'weather' and

because they indicate the position and anomalous intensity of convective activity associated with El Nino. Figure 5.17 shows annual rainfall at several Pacific Islands near the dateline; there are very large increases during El Nino events. These local changes may be put in a global context using satellite data as reported by Newman (1984). Figure 5.18 shows the percentage cover of cloud tops with radiative temperatures less than 235K on a 5° x 5° space scale for some recent northern hemisphere spring and winter seasons. This index is thought to give a good measure of convective activity. The data is not completely homogeneous in time but is probably spatially reasonably homogeneous. The relative minima in convection over the East Pacific are the result of the descending branch of the Walker cell. However by March-May 1983, highly anomalous heavy rainfall was reported from the semi-desert Galapagos Islands which turned green as a result; high SSTA persisted and even strengthened again in this region after the earlier mid summer peak around December/January 1982-3. Wright (1977) is also a useful reference for a number of observational aspects of SO.

5.1.4 AGCM Experiments

Is it physically reasonable that the global atmosphere could respond to El Nino? If so, how? Several experiments using AGCM's have been carried out using El Nino SST forcing; their results broadly support the idea of a widespread tropical response like that observed but give much more variable results in the extratropics (most of the experiments have concentrated on N Hemisphere teleconnections). The first N Hemisphere winter AGCM experiment, carried out by Rowntree (1972), indicated, like most subsequent experiments, that a pair of low level low pressure anomalies are forced on either side of the equator near the maximum tropical SSTA (probably nearer the local maximum absolute SST) with upper level anticyclones overlying the low pressure centres. Further north a nearby equivalent barotropic response occurs with a low anomaly forced at all levels well to the north of the tropical anomaly (about 35-50°N). The general result is to strengthen the Aleutian low. Palmer (1985) has recently carried out extensive experiments on El Nino using the Met Office 11-level AGCM for perpetual winter time conditions. Two of his experiments are discussed below:

5.1.4.1 Experiment 1 "Composite" El Nino SSTA

Palmer used a composite of the observed SSTA (Fig 5.19A) associated with several El Ninos (studied by RC) appropriate to December, but doubled in magnitude, with climatological SST elsewhere. Palmer carried out an anomaly experiment with this SSTA and a control experiment without it. Each experiment was continued for 540 model days using "perpetual" January radiation. Anomaly and control experiments both started from real atmospheric data for 28 December 1972, and the model incorporated "envelope" orography whereby mountains are enhanced in height to improve the model's winter climatology.

Fig 5.19B shows the average difference in 200 mb height (anomaly minus control) for these experiments. The "PNA" pattern of Horel and Wallace is evident and was found to be present at all levels. Tropical lows were overlain by tropical highs as expected (see Lecture 4 for a description of this upper level anticyclonic "vorticity" forcing). Tests showed that the

extratropical Rossby wave-like response was highly statistically significant.

5.1.4.2 Experiment 2 - December 1982 SSTA

The maximum of this real SSTA was to the east of the composite SSTA and simpler in shape (Fig 5.20a). Palmer used two versions of the 11-level AGCM integrated for perpetual winter conditions as before.

(a) Anomaly and control integrations using "envelope" orography, starting from 28 December 1972 atmospheric data.

(b) Anomaly and control integration for a model with "standard" orography, same starting date.

"Envelope" orography has higher mountains than "standard" orography. Both pairs of experiments were integrated for 540 model days.

Fig 5.20b show the difference between the anomaly and control experiments for (a) and (b). Neither figure shows a recognisable PNA pattern, and such a pattern was not in fact observed in 1982-83. Both models show a Rossby wave like anomaly response and in both pairs of experiments the response is highly statistically significant - but nevertheless different. In the "standard" orography experiment the anomaly wavelength is longer and the pattern is distorted compared to the "envelope" orography experiment. This is not surprising as the climatological mean flow of the "standard" orography model is much more westerly than that of the "envelope" model in winter, the "envelope" model being thought more realistic.

Conclusion from these experiments (and those of other workers) could be:-

(1) The wintertime extratropical response to El Nino may be quite strong but vary from event to event eg with the longitude or shape of the SSTA or position of the resulting absolute maximum tropical Pacific SST.

(2) The response of an AGCM will depend on its climatology. A realistic local response, as required for long-range forecasting, may demand a realistic representation of the structure of the mean flow.

5.1.5 Oceanographic aspects

Gill and Rasmusson (1983) have discussed the oceanographic aspects of the 1982-83 El Nino using a model of the response of the mixed layer of the tropical Pacific Ocean to the observed weakening of the trade winds near 160°E during early 1982. They assume a pre-existing (much as actually measured) gradient of sea surface topography with higher sea-level in the W Pacific than in the E Pacific (the east-west difference is typically observed to be about 1 m before El Nino and results from the wind stress imparted by the preceding strong SE trade winds). Fig 5.21 shows the longitude-time plots of eastward wind stress anomaly used in the model experiment, Fig 5.22A shows the computed change of surface elevation of the sea from a pre-existing condition where the height is greater in the west

and Fig 5.22B shows the resulting eastward ocean currents. These tend to oscillate in direction on a time scale of about 9 months as a result of the prediction of an eastward moving 'Kelvin' wave in the mixed layer which is partially reflected from the S American coast as a form of an equatorially trapped Rossby wave. Fig 5.23 shows the observed anomalies along the equator of (a) rainfall (measured by anomalies of outgoing long-wave radiation) (b) westerly wind (c) values of absolute SST (d) climatological average SST values. The model produced a good simulation of the observed change of sea-level topography and SSTA during ENSO; the sea level tends to rise first near the S American coast but the main warming of SST propagates eastwards from the W toward the central Pacific, though warming is initiated almost simultaneously near S America too. So there is much more to be understood about El Nino as this behaviour, though correct for 1982-3, is not always typical.

Conclusion

The ENSO event represents the most important non-seasonal, if irregularly recurring, event in the climate system on time scales between the annual cycle and the ice ages that has yet been properly identified. The factors that initiate the El Nino/ENSO sequence remain elusive. Some of the physical processes that occur in the ocean and the atmosphere during ENSO have nevertheless been isolated.

REFERENCES TO ADVANCED LECTURE 5 PART I

ANGELL, J K (1981) Comparison of variations in atmospheric quantities with sea surface temperature variations in the equatorial eastern Pacific. Mon Weath Rev, 109, pp 230-243.

BACASTOW, R B AND KEELING, C D (1981) Atmospheric CO_2 and the Southern Oscillation; effects associated with recent El Nino events. Proc WMO/ICSU/UNEP Conf on Analysis and Interpretation of Atmospheric CO_2 data, pp 109-112. WCP-14, Geneva.

BERLAGE, H P (1966) The Southern Oscillation and world weather. Mededel. Verhandel. 88, Kon Ned Met Inst, 152 pp.

BERLAGE, H P AND DE BOER, H J (1959) On the extension of the Southern Oscillation throughout the world during the period July 1 1949-July 1 1957. Geofis Pure Appl, 44, pp 287-295.

BJERKNES, J (1969) Atmospheric teleconnections from the equatorial Pacific. Mon. Weath. Rev., 97, pp 163-172.

CHEN, W Y (1982) Fluctuations in northern hemisphere 700 mb height field associated with the Southern Oscillation. Mon Weath Rev, 110, pp 808-823.

FOLLAND, C K; PARKER, D E AND NEWMAN, M R (1985) Worldwide marine temperature variations on the season-to-century time scale. Proc 9th Climate Diagnostics Conf, Corvallis, Oregon, 22-26 Oct 1984, pp 70-85.

GILL, A E AND RASMUSSON, E M (1983) The 1982-83 climate anomaly in the equatorial Pacific. Nature, 306, pp 229-234.

GODBOLE, R V AND SHUKLA, J (1981) Global analysis of January and July sea level pressure. NASA Tech Mem 82097, Goddard Space Flight Center, Greenbelt, Maryland 20771.

HOREL, J D (1982) On the annual cycle of the tropical Pacific atmosphere and ocean. Mon Weath Rev, 110, pp 1863-1878.

HOREL, J D AND WALLACE, J M (1981) Planetary scale atmospheric phenomena associated with the Southern Oscillation. Mon Weath Rev, 109, pp 813-829.

KOUSKY, V E; KAGANO, M T AND CAVALCANTI, I F A (1984) A review of the Southern Oscillation: oceanic-atmospheric circulation changes and related rainfall anomalies. Tellus, 36A, pp 490-504.

MARYON, R H AND STOREY, A M (1985) A multivariate statistical model for forecasting anomalies of half-monthly mean surface pressure. J Clim, 5, pp 561-578.

MOSSMAN, R C (1924) Indian monsoon rainfall in relation to South American weather, 1875-1914. Mem Ind Met Dept, 23, pp 157-242.

NEWMAN, M R (1984) Observational aspects of the El Nino and the atmospheric response. Met O 13 Branch Memo 148.

PALMER, T N (1985) A General Circulation Model's response to sea surface temperature anomalies in the tropical Pacific Ocean. Proc 16th Liege Conf on Ocean Hydrodynamics. Elsevier Sc Pub, Amsterdam.

PAN, Y H AND OORT, A H (1983) Global climate variations connected with sea surface temperature anomalies in the eastern equatorial Pacific Ocean for the 1958-73 period. Mon Weath Rev, 111, pp 1244-1258.

PARKER, D E (1983) Documentation of a Southern Oscillation index. Met Mag, 112, pp 184-188.

PHILANDER, S G H (1985) El Nino and La Nina. J Atm Sci, 42, pp 2652-2662.

QUIROZ, R S (1983) The climate of the "El Nino" winter of 1982-83 - a season of extraordinary climatic anomalies. Mon Weath Rev, 11, pp 1685-1706.

RASMUSSON, E M AND CARPENTER, T H (1982) Variations in tropical sea surface temperature and surface wind fields associated with the Southern Oscillation/El Nino. Mon Weath Rev, 110, pp 354-384.

ROWNTREE, P R (1972) The influence of tropical east Pacific Ocean temperatures on the atmosphere. Q J Roy Met Soc, 98, pp 290-321.

SELKIRK, R (1984) Seasonally stratified correlations of the 200 mb tropical wind field to the Southern Oscillation. J Clim, 4, pp 365-382.

SHUKLA, J AND PAOLINO, D A (1983) The Southern Oscillation and long-range forecasting of the summer monsoon rainfall over India. Mon Weath Rev, 111, pp 1830-1837.

VAN LOON, H, ZEREFOS, C S AND REPAPIS, C C (1982) The Southern Oscillation in the Stratosphere. Mon Weath Rev, 110, pp 225-229.

WRIGHT, P B (1977) The Southern Oscillation - patterns and mechanisms of the teleconnections and the persistence. Grant OCE-76-23173, University of Hawaii.

WYRTKI, K (1975) El Nino - the dynamic response of the equatorial Pacific Ocean to atmospheric forcing. J Phys Ocean, 5, pp 572-584.

ADVANCED LECTURE NO. 5

PART II - QUASI-BIENNIAL OSCILLATION

C K FOLLAND AND D E PARKER

5.2.1 Introduction

A brief description is given of this curious lower-stratospheric phenomenon which was discovered almost simultaneously by Ebdon (1960) and Reed (1960). The QBO is the only quasi-periodic process of reasonably regular behaviour known in the climate system whose time scale lies between the annual and ice-age time scales. (The next most regular process is the ENSO phenomenon discussed in Pt I). Although the links between QBO and surface climate are tenuous, (though often suggested), we justify its inclusion here:-

(a) to provide a background to the description of volcanic dust and climate in lecture 3; the QBO affects our ability to interpret and detect the effects of volcanic dust on stratospheric temperature and thus to unravel the physical properties of volcanic dust

(b) because of the possibility of a link with the ENSO events and, perhaps, other climate anomalies that may be confirmed in the future.

5.2.2 Description

QBO shows up most prominently as a quasi-biennial oscillation of wind direction, speed and temperature in the tropical lower stratosphere within 15° of the equator. Fig 5.24A shows the monthly mean 30 mb winds above Canton Island (central Pacific) 1954-1967, Gan (Central Indian Ocean) 1967-75, Singapore 1976-81 and Changi 1981 onwards. Corresponding 50 mb winds are shown in Fig 5.24B. The associated temperature changes between 50 mb, and 150 mb (where they disappear) are shown in Fig 5.25. It is possible to form composite time series from such widely-separated tropical stations because the QBO occurs on a global scale in the tropics with very little phase-lag between different longitudes (at a given elevation). The period of the QBO is not constant: it varies from less than 2 years to about 3 years, and averages 2 years and 3 months. Periods close to either 2 or 3 years tend to be favoured, and there are also favoured seasons for reversal of the 50 mb or 30 mb wind directions (Parker 1976). A downwards phase propagation of the oscillation occurs; for example, changes in the 50 mb wind vector lag several months behind similar changes in the 30 mb wind vector (Fig 5.26).

The discovery of the tropical stratospheric QBO has been followed by widespread reports of quasi-biennial behaviour in local tropospheric climate and circulation parameters. Parthasarathy and Mooley (1978) found a quasi-biennial oscillation in Indian Monsoon rainfall, but this was not strong and regular enough to be used for forecasting. Ebdon (1975) documented differences in the mean Northern hemisphere mid-latitude surface pressure and 500 mb geopotential patterns, and in zonal winds aloft, that varied according to the phase of the tropical QBO. Figure 5.27 illustrates the mean sea level pressure anomaly in the extratropical N Hemisphere for Julys with a westerly tropical QBO wind mode. The anticyclonic anomaly

near the British Isles was found to be statistically significant at about the 5% level. In addition, not only Ebdon (1975) but also Angell and Korshover (1977) observed that the circumpolar upper-tropospheric vortex was smaller during the westerly phase of the QBO, particularly in winter, with an associated increase of tropospheric temperature of several tenths °C in mid-latitudes. Consequent possible associations with, for example, summer temperature and sunshine in the United Kingdom, were noted by Ebdon and also by Folland (1977). Holton and Tan (1980) (Fig 5.28) have demonstrated that there may be a 50 mb and a 1000 mb quasi-biennial oscillation in the geopotential and temperature of the northern polar regions. The two atmospheric levels oscillate in phase but the amplitude is weaker at 1000 mb. It must be emphasised that observations of QBO outside the tropical stratosphere have been associated only statistically with the tropical stratospheric QBO at this stage. Physical associations have not been established.

The physical causes of the tropical stratospheric QBO were studied in a quite convincing paper by Holton and Lindzen (1972) but since then evidence has mounted which casts serious doubt on their hypothesis and currently much research is going on. So we will not describe the theories here.

The mechanisms by which the tropical lower stratospheric quasi-biennial oscillation might affect the rest of the atmosphere are completely uncertain. It is just possible that the associated temperature changes near the tropical tropopause (Fig 5.25) may affect the strength of tropical convection where it is most powerful eg the tropical W Pacific, and thereby influence the Hadley or Walker cells and subsequently the rest of the circulation. It is known that tropospheric air almost certainly regularly enters the stratosphere in this region (Newell and Gould-Stewart (1981)).

5.3 Angular momentum considerations

It is worth mentioning that in N Hemisphere summer the difference in the axial angular momentum of the N Hemisphere atmosphere contributed to by a maximum westerly phase of QBO compared to a maximum easterly phase may sometimes be 5%-10% of the total N Hemisphere axial angular momentum (allowing for phase lags of the QBO with height). In any case the development of a westerly phase of QBO represents an increase in the axial momentum of the atmosphere where it is already by definition a maximum. So small, compensating changes in atmospheric circulation that preserve axial angular momentum should occur somewhere else (in either hemisphere). Note that this momentum cannot be transmitted to and temporarily stored or released in earth's rotation in a direct way as the stratospheric wind oscillation occurs well above the level of any mountains, though this transfer could occur indirectly through a tropospheric circulation change.

REFERENCES TO ADVANCED LECTURE 5 PART II

ANGELL, J K AND KORSHOVER, J (1977) Variation in size and location of the 300 mb north circumpolar vortex between 1963 and 1975. Mon Weather Rev, 105, pp 19-25.

EBDON, R A (1960) Notes on the wind flow at 50 mb in tropical and sub-tropical regions in January 1957 and January 1958. Q J Roy Met Soc, 86, pp 540-542.

EBDON, R A (1975) The quasi-biennial oscillation and its association with tropospheric circulation patterns. Meteorol Mag, 104, pp 282-297.

FOLLAND, C K (1977) Recent work on some quasi-cyclic fluctuations of meteorological parameters affecting British climate. Weather, 32, pp 336-342.

HOLTON, J R AND LINDZEN, R S (1972) An updated theory for the quasi-biennial cycle of the tropical stratosphere. J Atm Sci, 29, pp 1076-1080.

HOLTON, J R AND TAN, H-C (1980) The influence of the equatorial quasi-biennial oscillation on the global circulation at 50 mb. J Atm Sci, 37, pp 2200-2208.

NEWELL, R E AND GOULD-STEWART, S (1981) A stratospheric fountain? J Atm Sci, 38, pp 2789-2796.

PARKER, B N (1976) The quasi-biennial oscillation in tropical stratospheric winds: a method of forecasting. Meteorol Mag, 105, pp 134-143.

PARTHASARATHY, B AND MOOLEY, D A (1978) Some features of a long homogeneous series of Indian summer monsoon rainfall. Mon Weather Rev, 106, pp 771-781.

REED, R J (1960) The circulation of the stratosphere. Paper presented at the 40th Annual meeting of the American Met Soc, Boston, Mass.

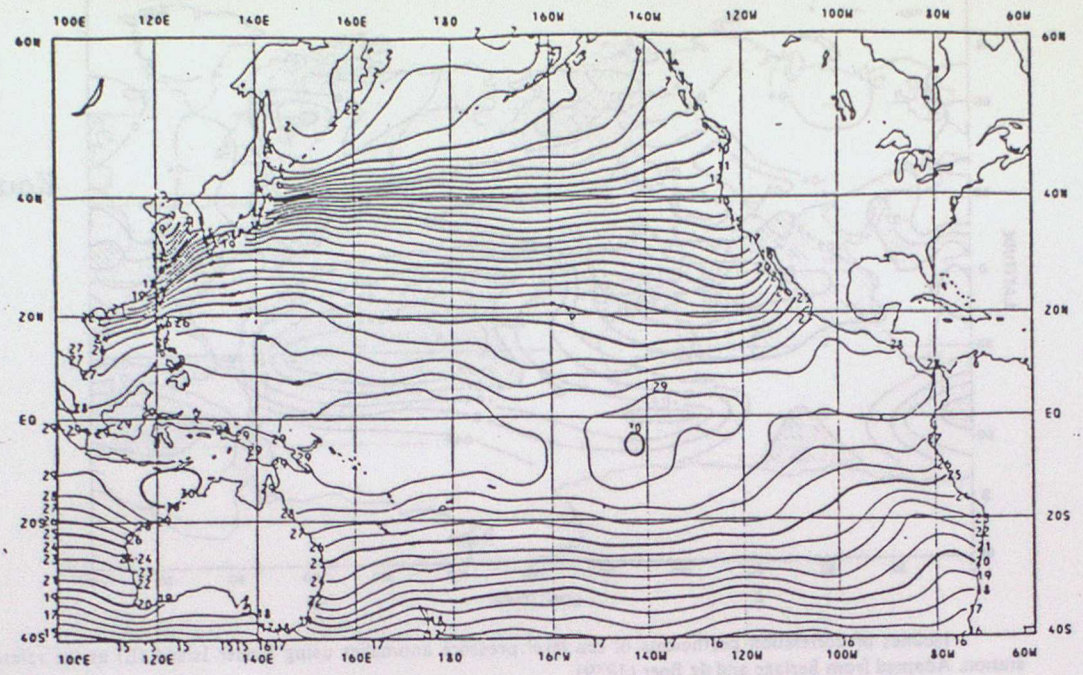

Figure 5.1

From Quiroz(19

. Sea surface temperature over the Pacific Ocean for winter 1982–83.

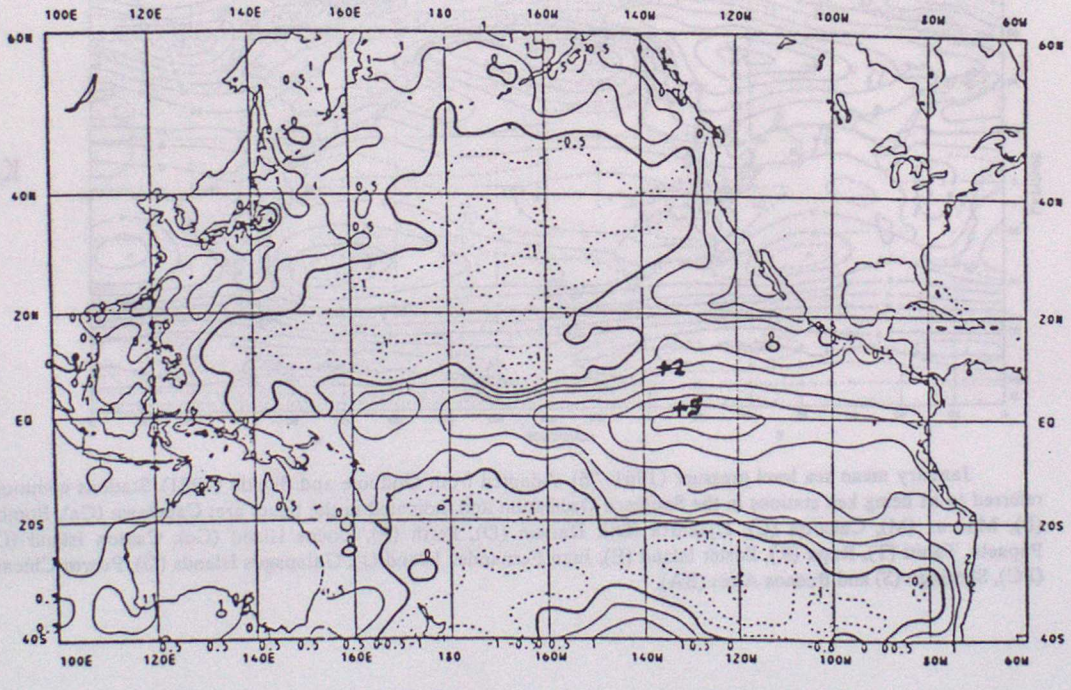

Figure 5.

From Quiroz(1983

Sea surface temperature (°C) for winter 1982–83 over the Pacific Ocean. Dashed lines portray negative anomalies, thin solid lines indicate positive anomalies, and the heavy solid line is the zero line. Anomalous isotherms are at 1°C intervals except for 0.5°C between +1 and −1°C.

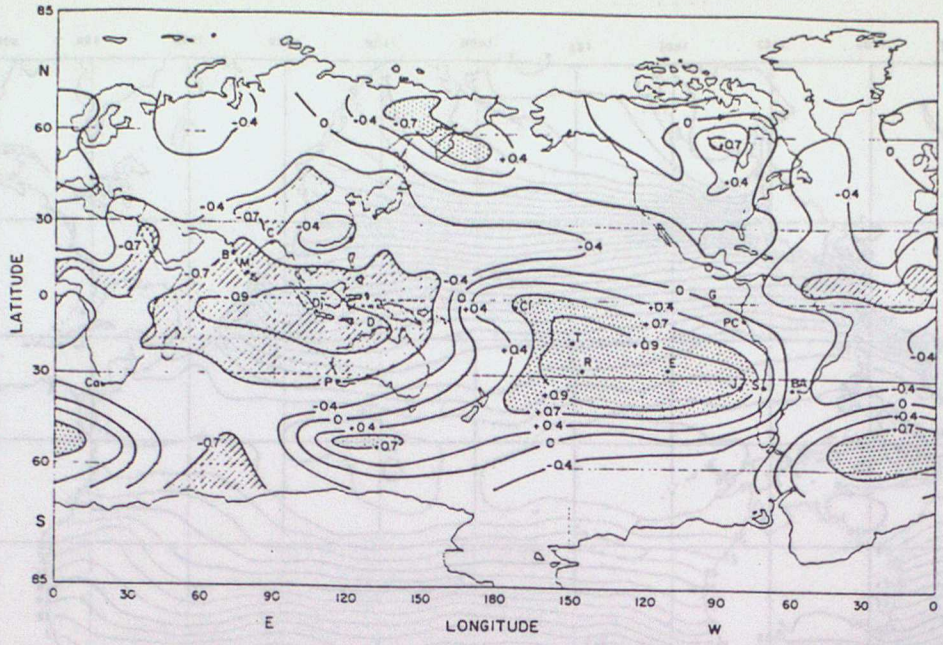

Figure 5.3.

From Kousky et al (1984).

Isolines of correlation coefficients of sea level pressure anomalies using Easter Island (E) as the reference station. Adapted from Berlage and de Boer (1959).

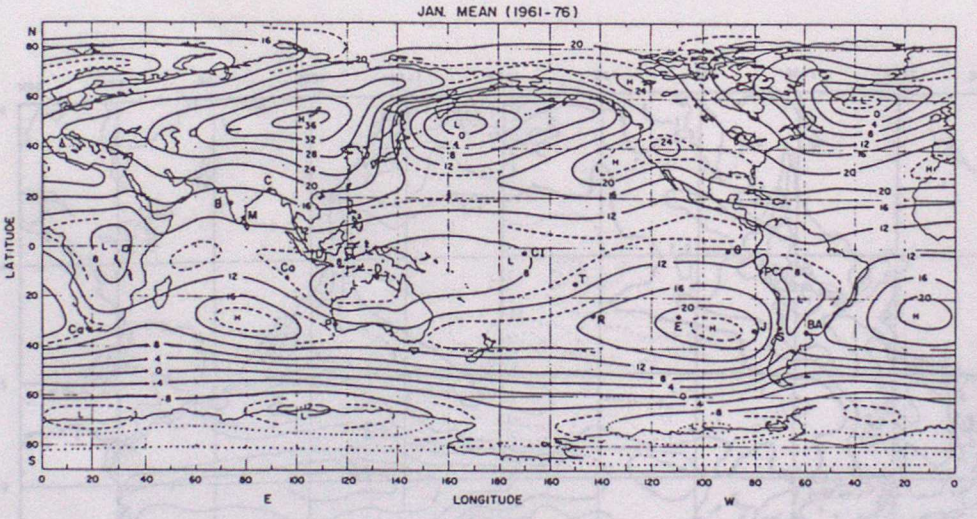

Figure 5.4

From Kousky et al (1984).

January mean sea level pressure (1961–76). Adapted from Godbole and Shukla (1981). Stations commonly referred to as being key stations in the Southern Oscillation and indicated in the figure are: Capetown (Ca), Bombay (B), Madras (M), Calcutta (C), Djakarta (Dj), Darwin (D), Perth (P), Cocos Island (Co), Canton Island (CI), Papaete, Tahiti (T), Rapa (R), Easter Island (E), Juan Fernandez Island (J), Galapagos Islands (G), Puerto Chicama (PC), Santiago (S) and Buenos Aires (BA).

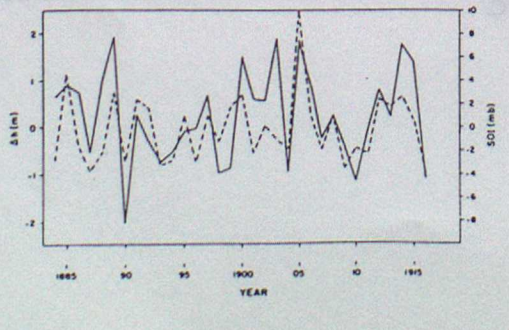

The mean Parana river level anomalies (m), for April–September, at Rosario, Argentina (dashed line) and a Southern Oscillation Index (SOI) (solid line) calculated by taking the sum of the pressure anomalies (mb) at Bombay, Madras, Djakarta, Calcutta, Darwin, Perth and Cape Town for the period of October–March. The SOI values are plotted in the year corresponding to the January–March period, and are taken from Berlage (1966). The Parana river level anomalies are taken from Mossman (1924).

Figure 5.5. From Kousky et a (1984).

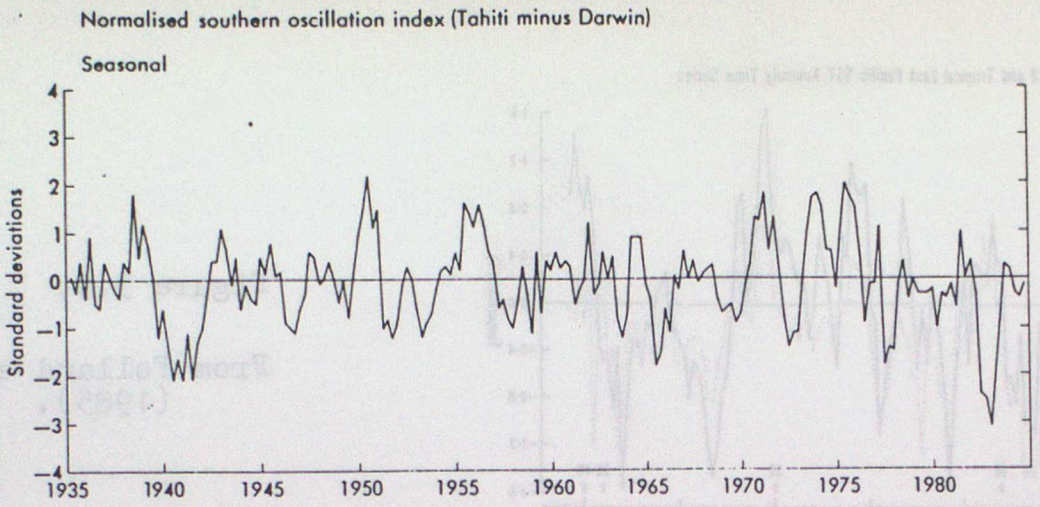

Figure 5.6.

SEASONAL SST AND MATN ANOMALIES FROM 1856 WITH RESPECT TO 1951-60 MEANS AVERAGED OVER THE EAST TROPICAL PACIFIC: SOLID LINE IS MATN ANOMALY - DASHED LINE IS SST ANOMALY (MATN is night marine air temperature).

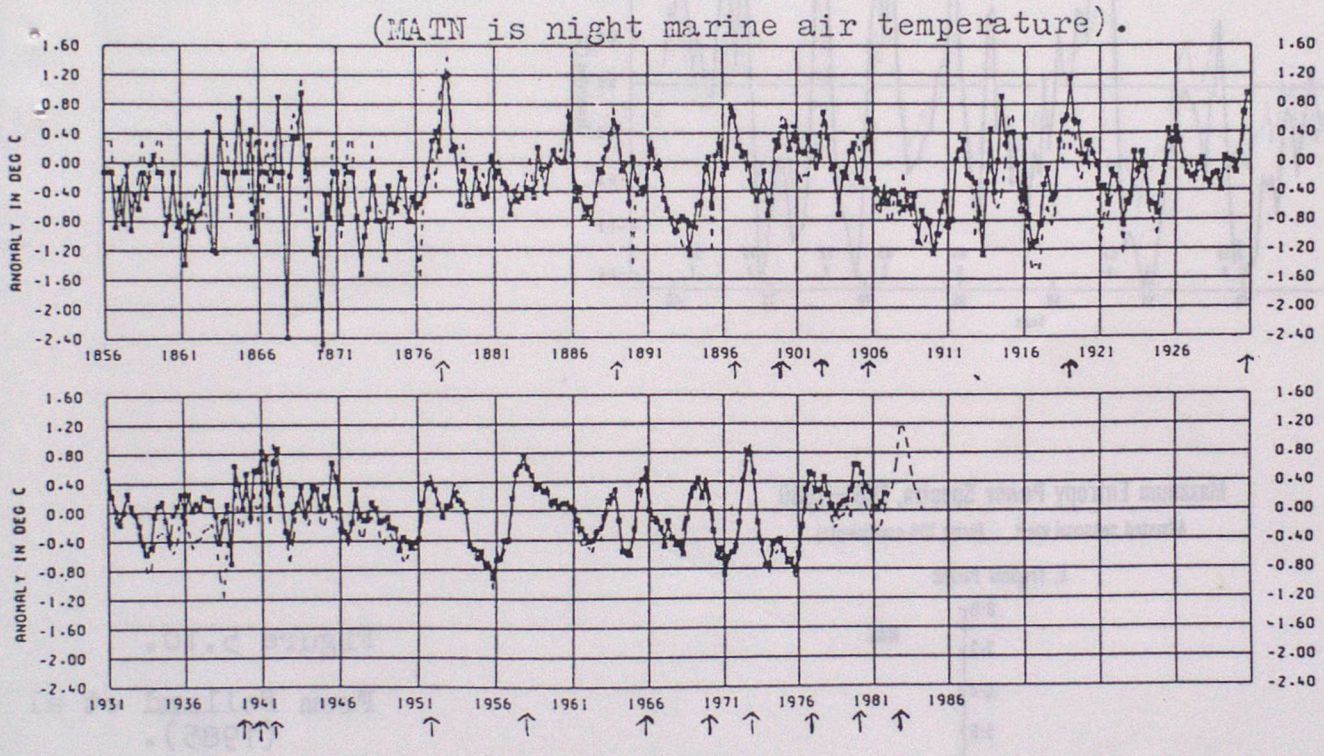

Arrows mark Oct-Dec of El Nino years

Figure 5.7.

From Folland et al (1985).

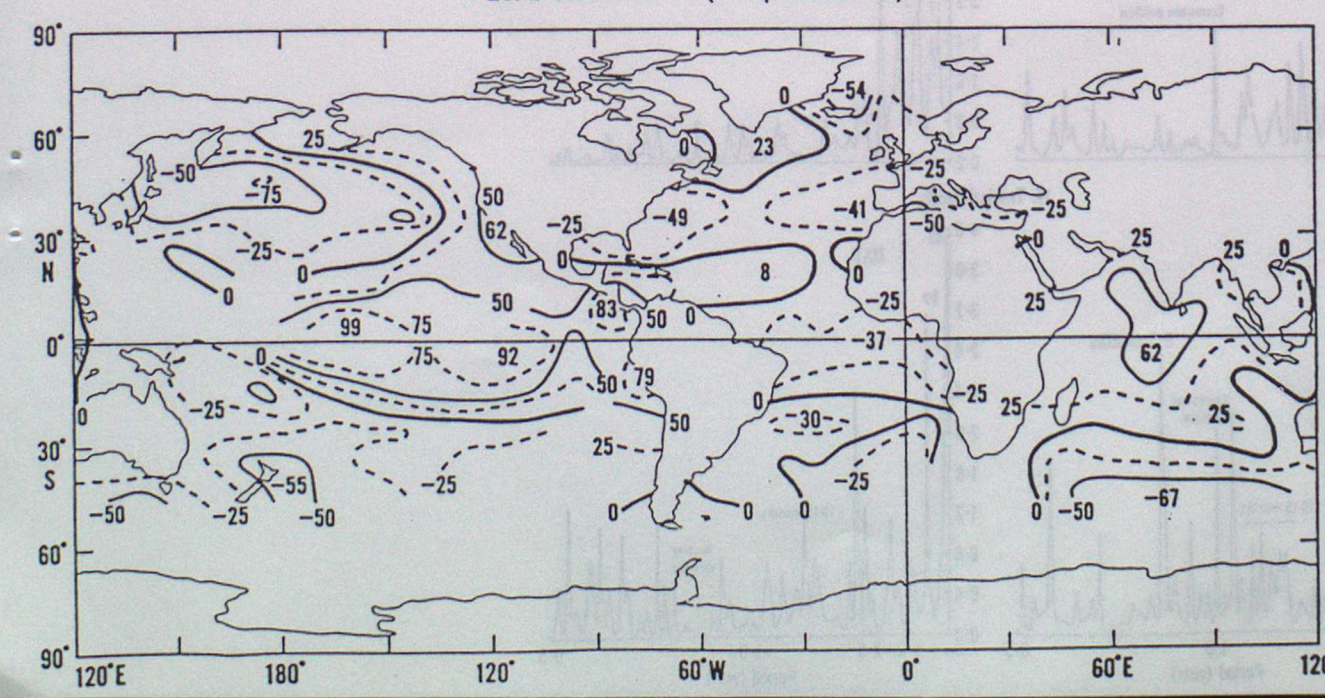

Figure 5.

From Folland et al (1985)

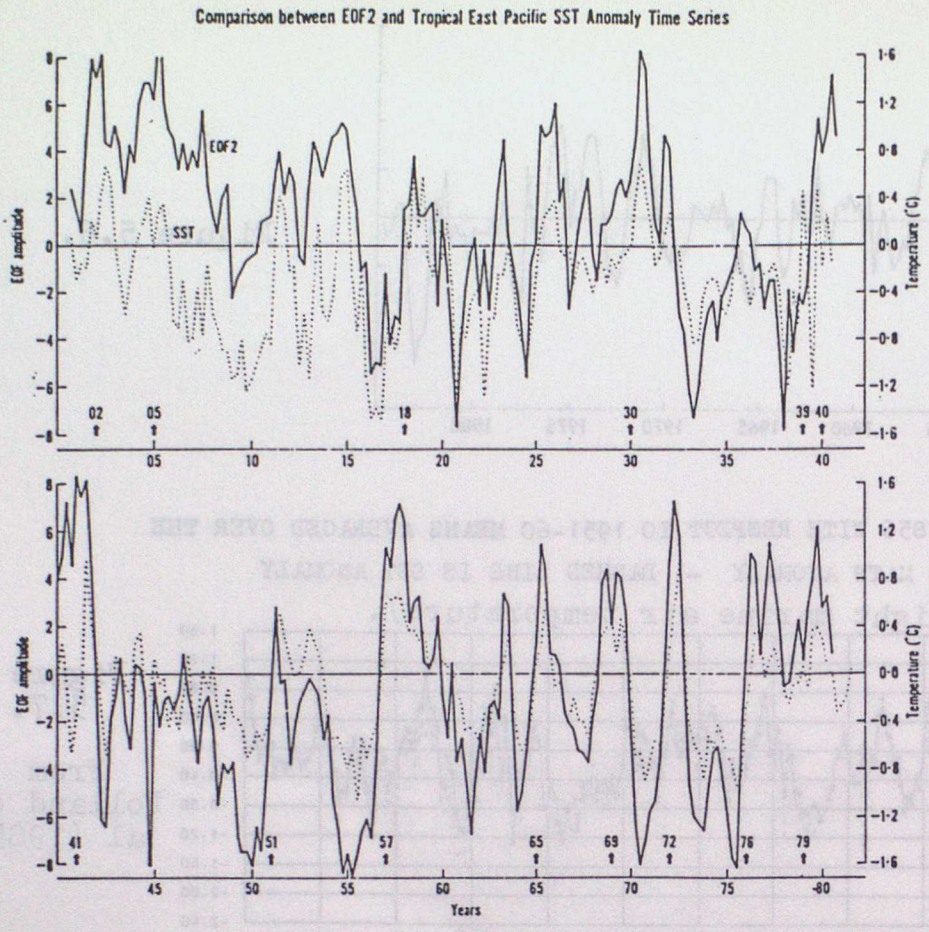

Figure 5.9.

From Folland et al (1985).

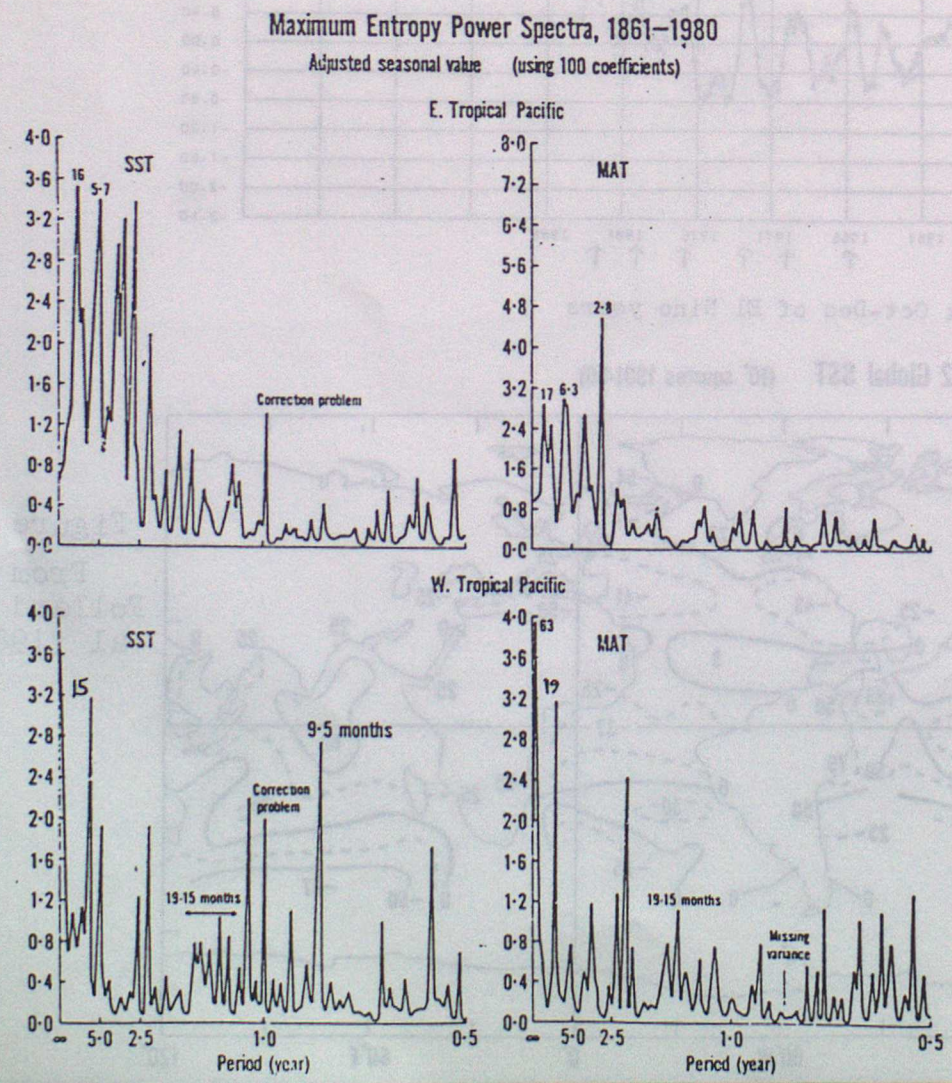

Figure 5.10.

From Folland et al (1985).

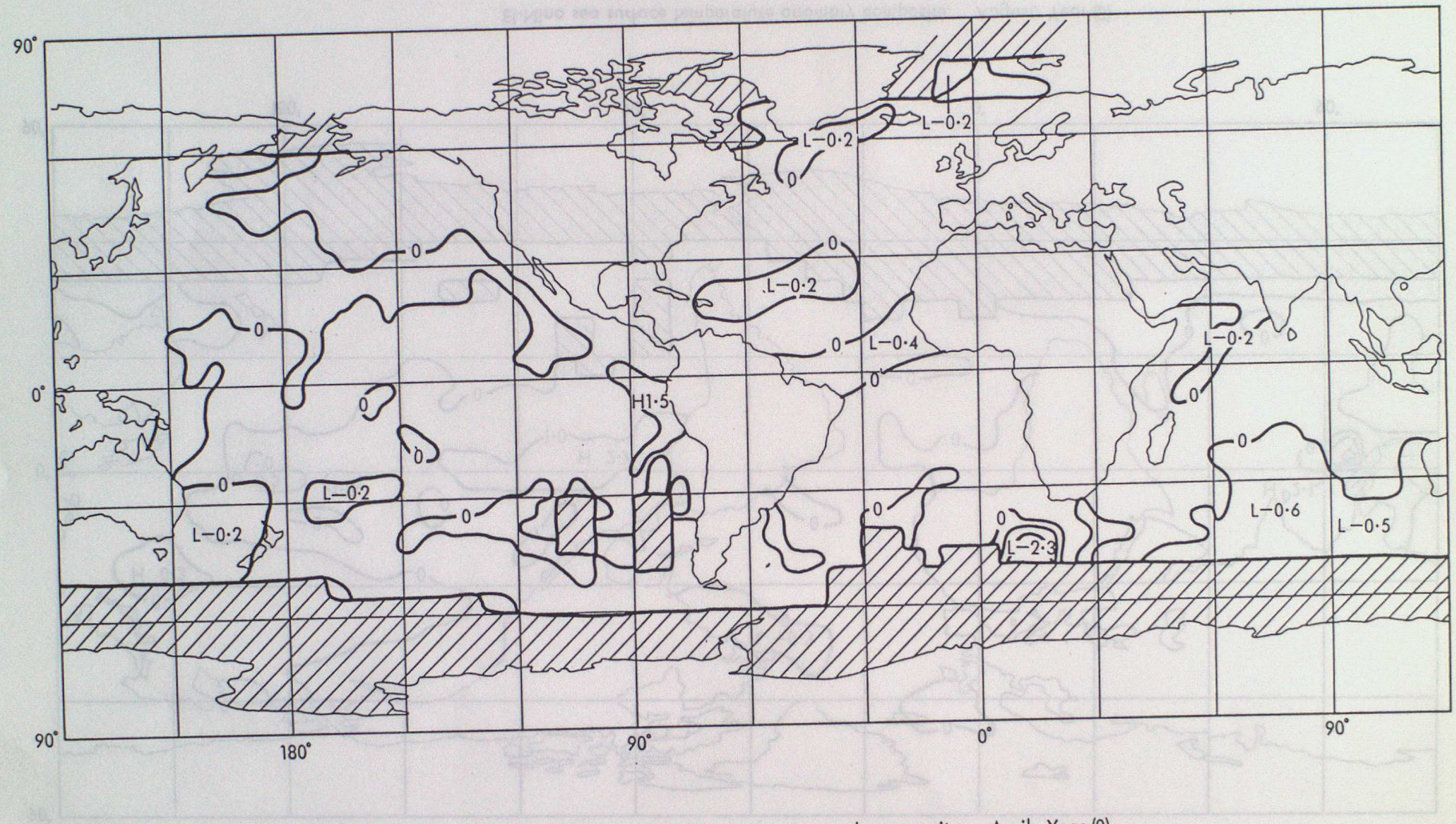

El-Nino sea surface temperature anomaly composite. April , Year (0)

Figure 5.11A. From Newman (1984).

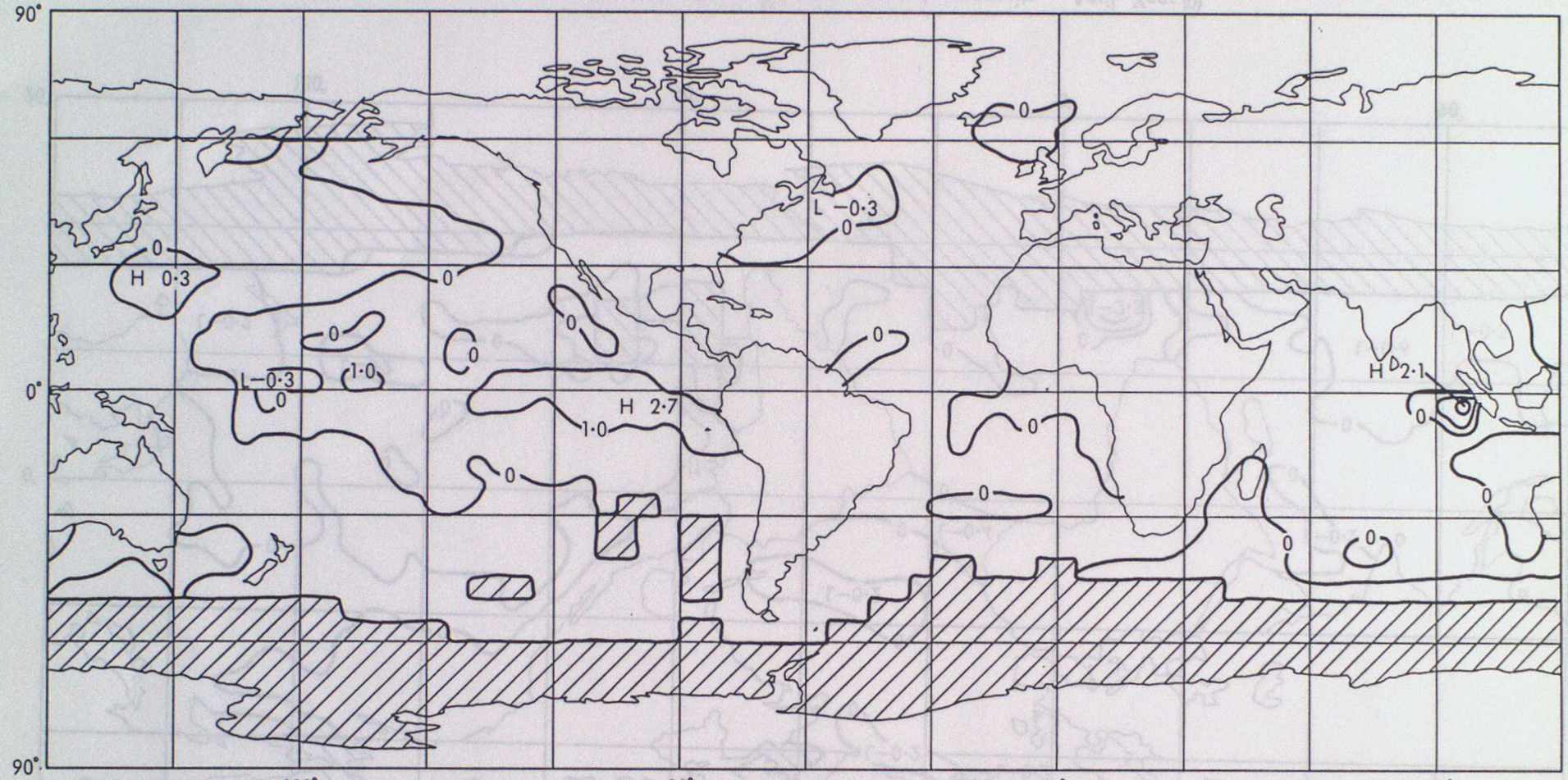

El-Nino sea surface temperature anomaly composite. August, Year (0)

Figure 5.11B. From Newman (1984).

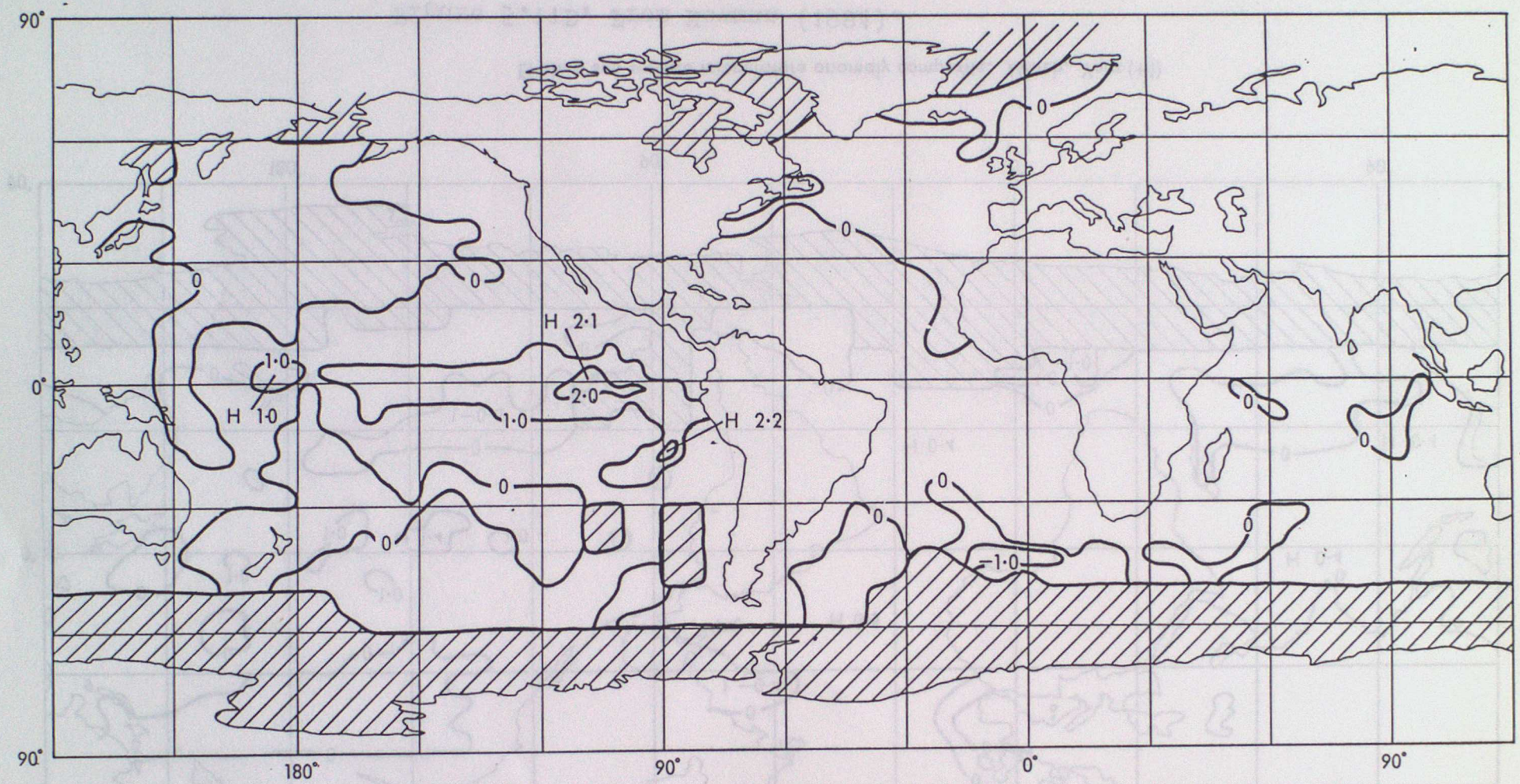

El-Nino sea surface temperature anomaly composite. December, Year (0)

Figure 5.11C. From Newman (1984).

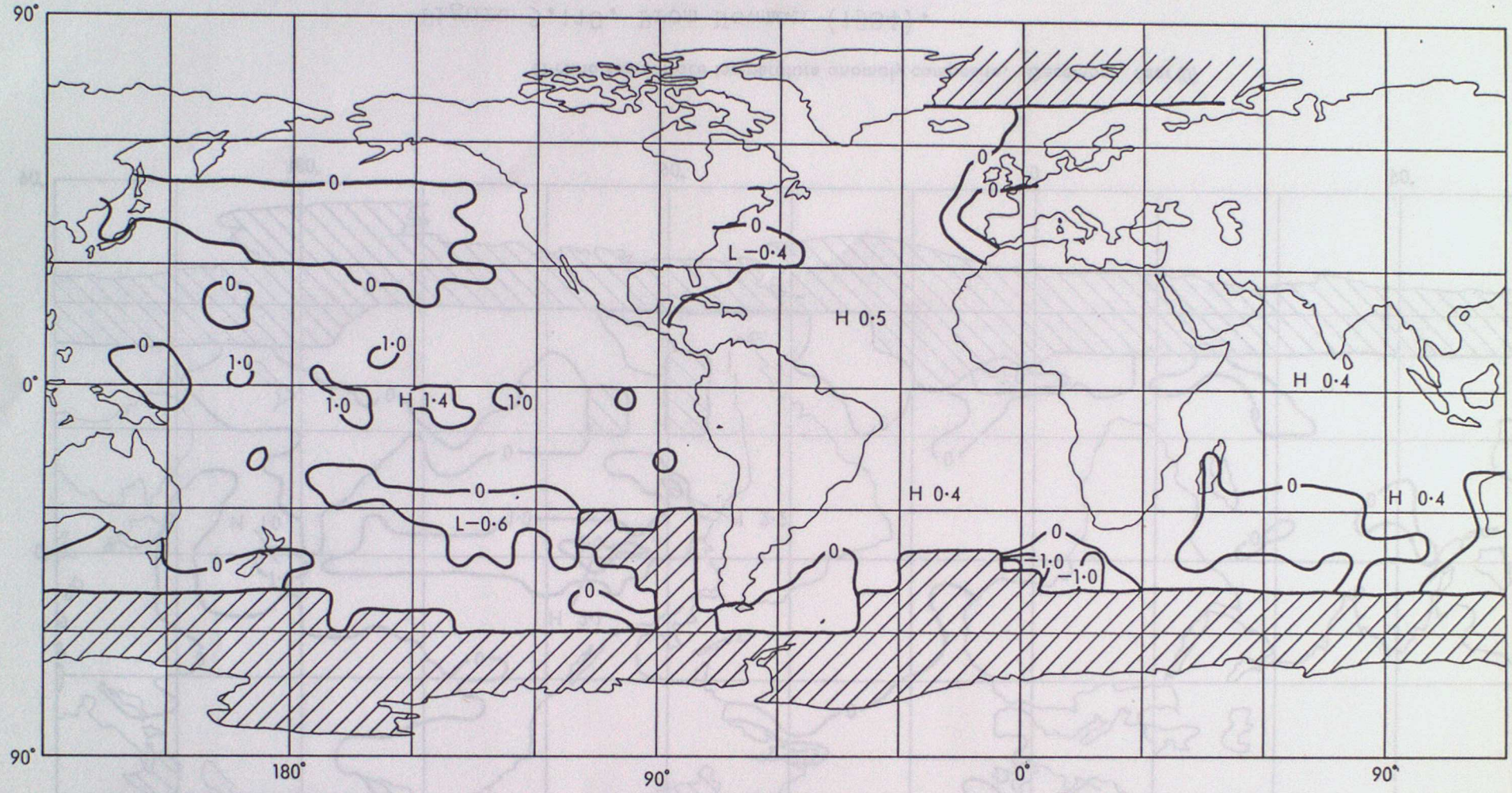

El-Nino sea surface temperature anomaly composite. March, Year (+1)

Figure 5.11D. From Newman (1984).

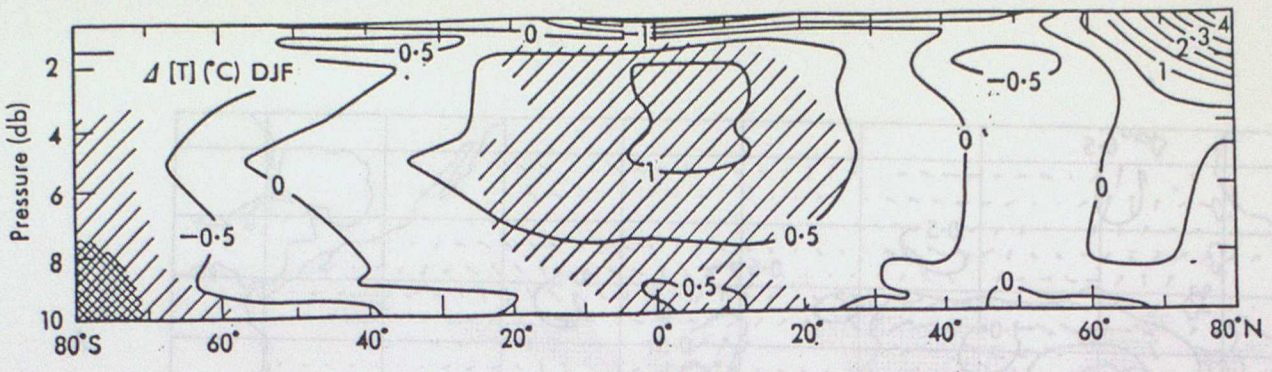

Zonal mean cross section of the average temperature difference (°C) between cases when the winter mean surface temperatures at 2·5°S, 130°W was relatively warm and cases when it was relatively cool. (After Pan & Oort, 1983).

Figure 5.12.

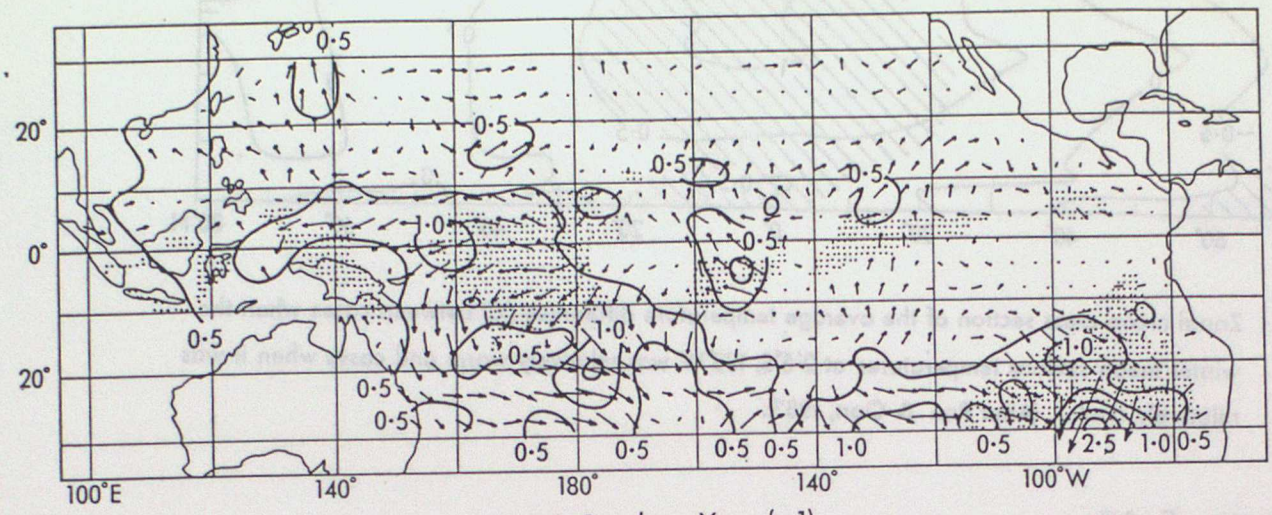

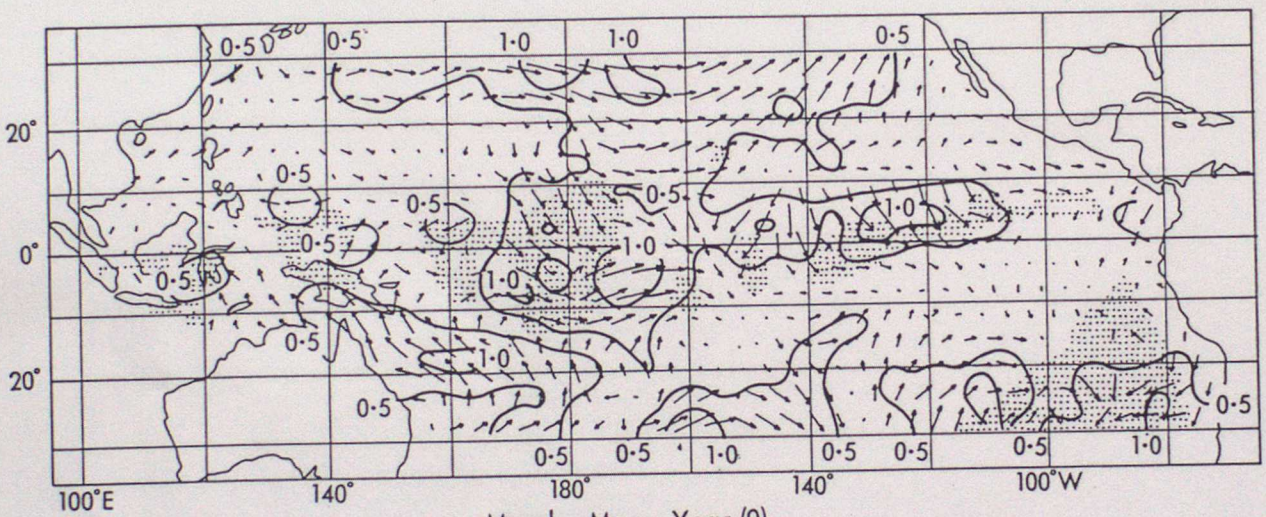

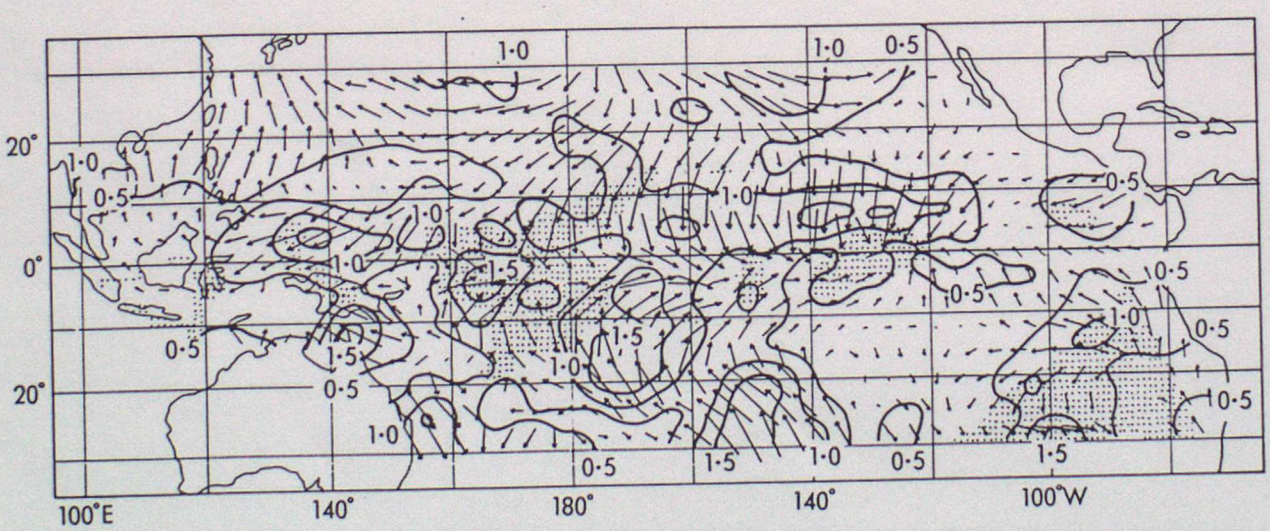

El-Nino surface wind anomaly composites (units m s^{-1}).

Areas in which the number of observations average less than 10 in a two degree square are shaded on the wind composite.

Figure 5.13. After Rasmusson and Carpenter (1982).

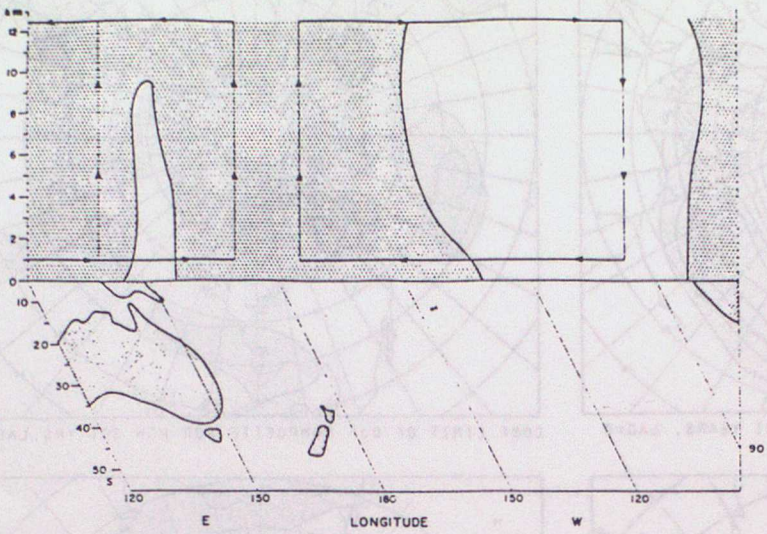

Figure 5.14.
From Kousky et al (1984).

. Schematic diagram of the Pacific Walker Circulation. Shaded regions are areas of rising motion. The circulation pattern shown is the January mean for 1979–81

(Figure 5.15 follows Figure 5.16).

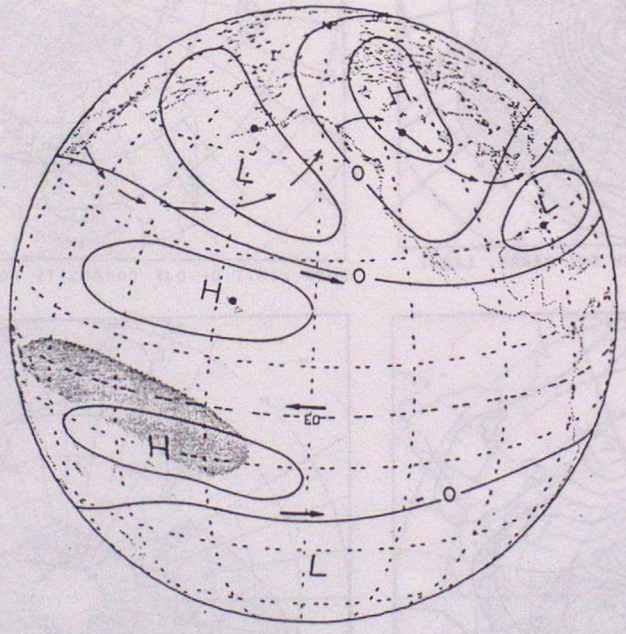

Figure 5.16.

From Horel and Wallace (1981).

. Schematic illustration of the hypothesized global pattern of middle and upper tropospheric geopotential height anomalies (solid lines) during a Northern Hemisphere winter which falls within an episode of warm sea surface temperatures in the equatorial Pacific. The arrows in darker type reflect the strengthening of the subtropical jets in both hemispheres along with stronger easterlies near the equator during warm episodes. The arrows in lighter type depict a mid-tropospheric streamline as distorted by the anomaly pattern, with pronounced "troughing" over the central Pacific and "ridging" over western Canada. Shading indicates regions of enhanced cirriform cloudiness and rainfall. For further details see Section 7. The locations of the stations used in Table 4 are indicated by dots.

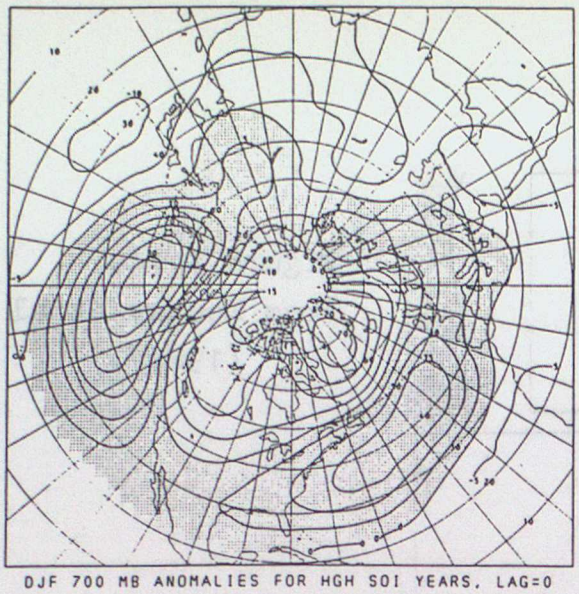

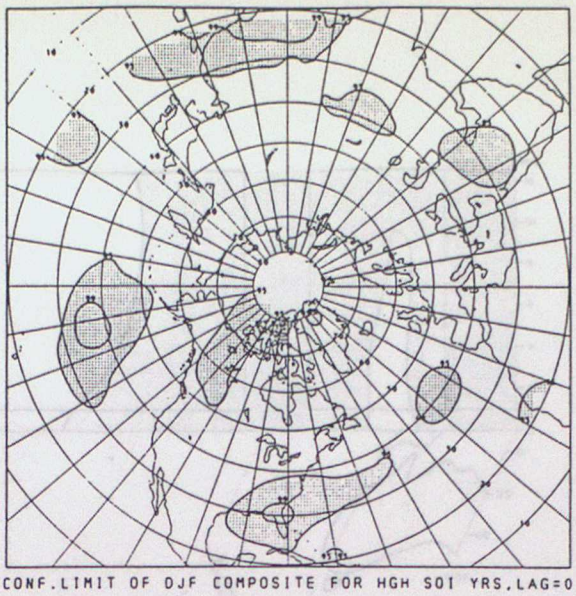

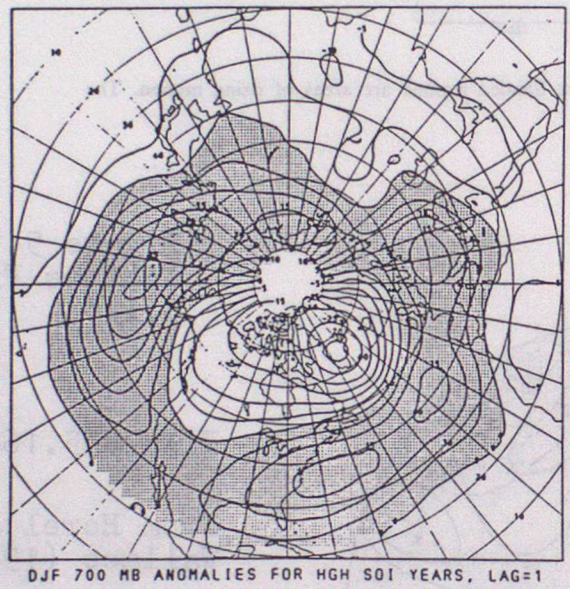

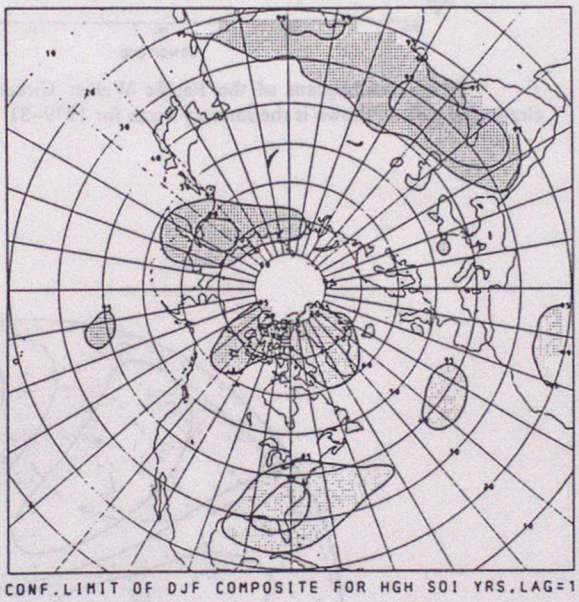

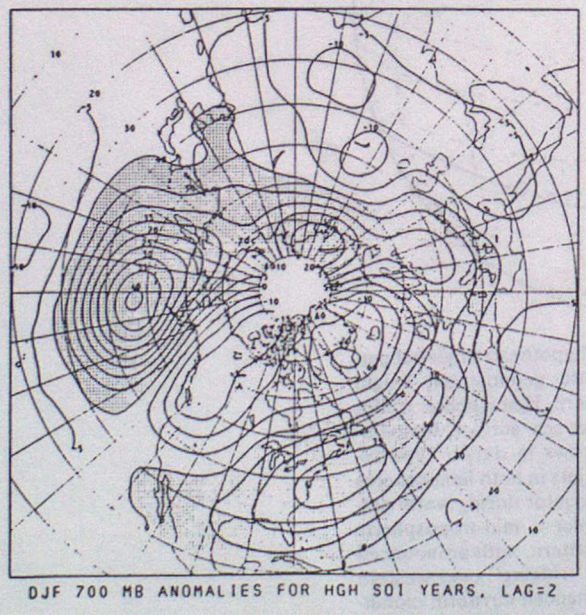

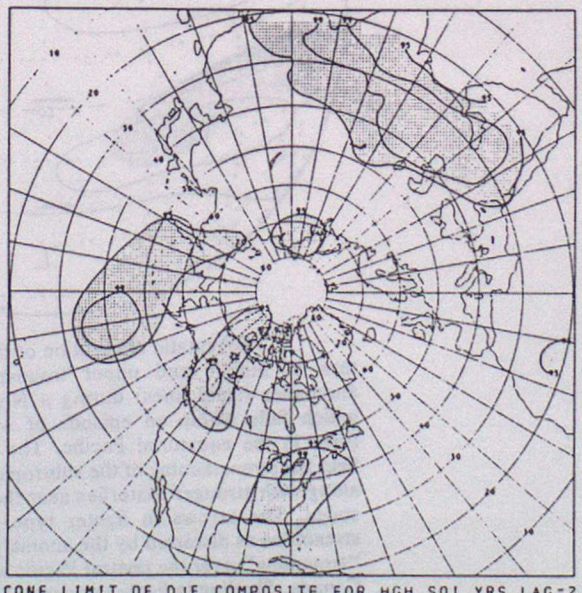

FIG. 7. Winter composites associated with high SOI values with the latter leading the height field by various seasons. The shaded areas are positive and the contour interval is 5 m. Confidence limits of the anomalies are presented on the right.

Figure 5.15A. From Chen(1982).

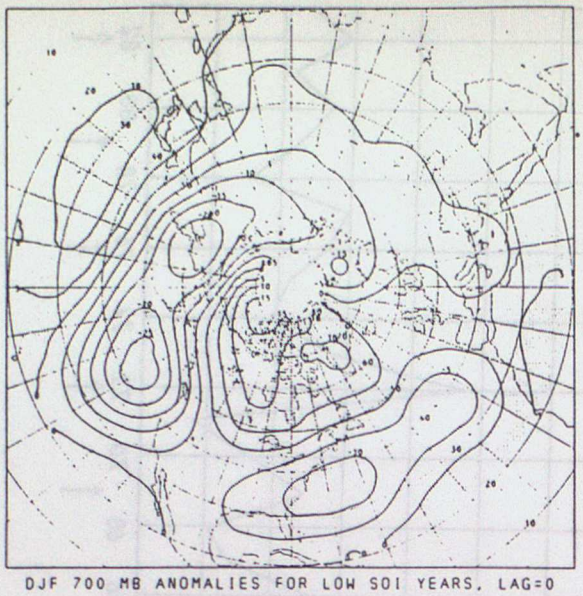

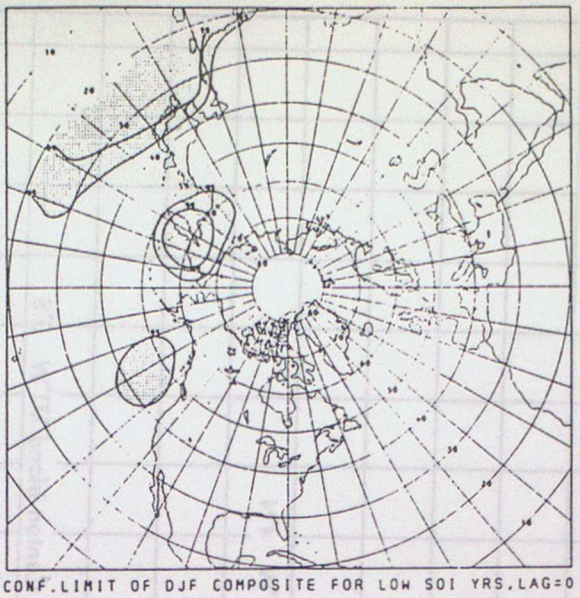

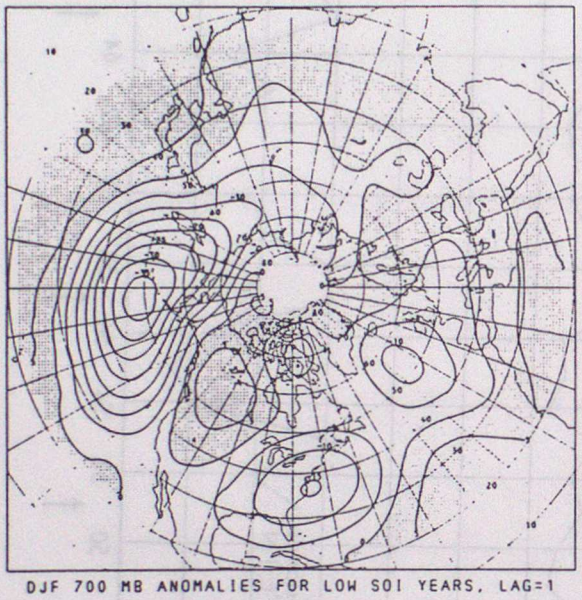

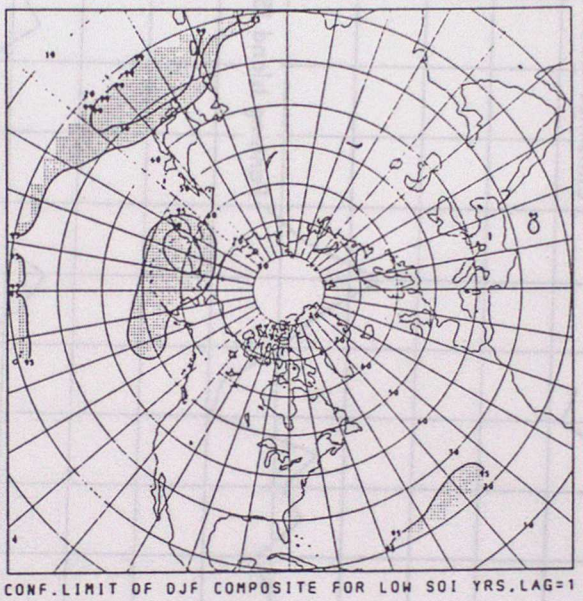

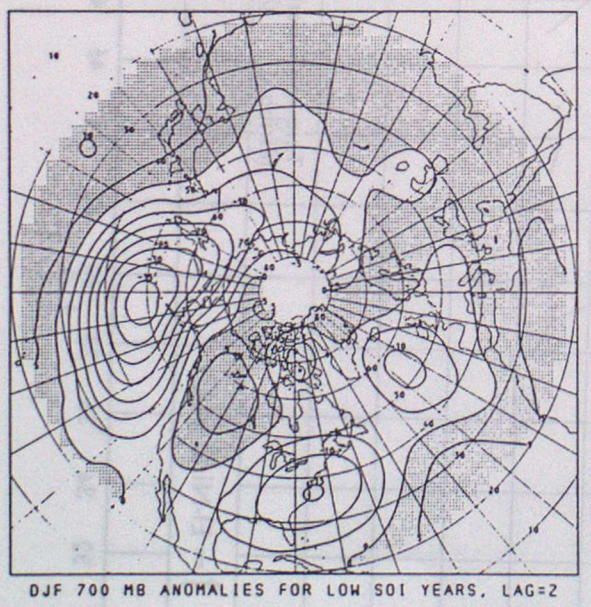

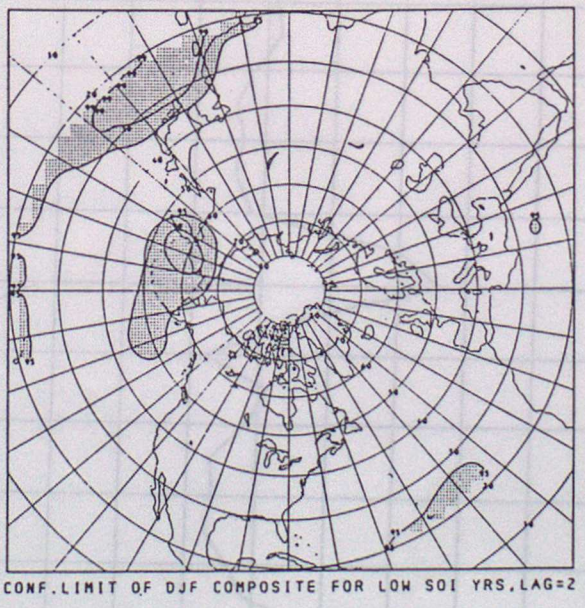

Figure 5.15B. As Fig. 5.15A, but for low SOI values. From Chen (1982).

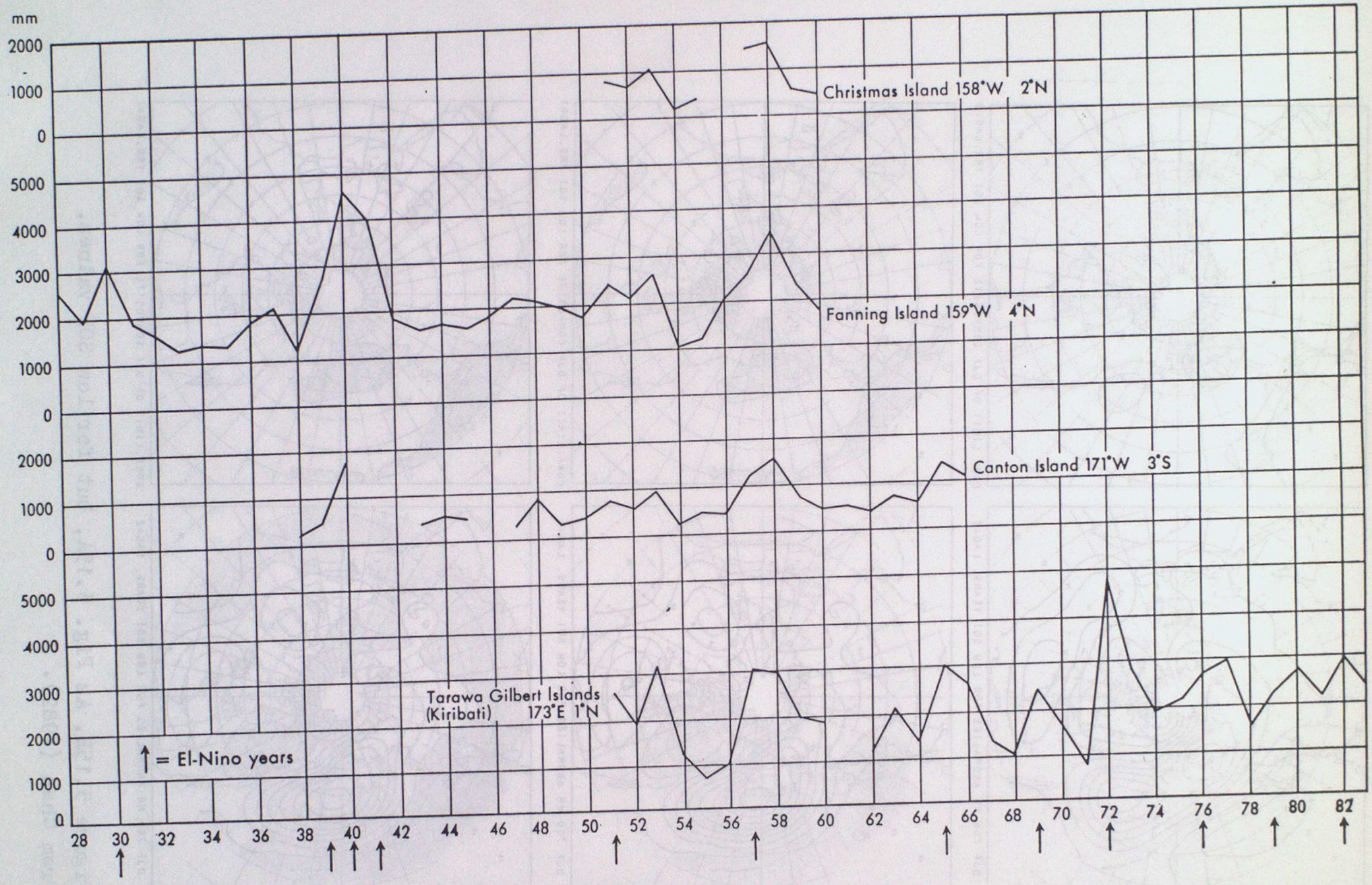

Figure 5.17 Annual rainfall at selected Pacific islands
From Newman (1984)

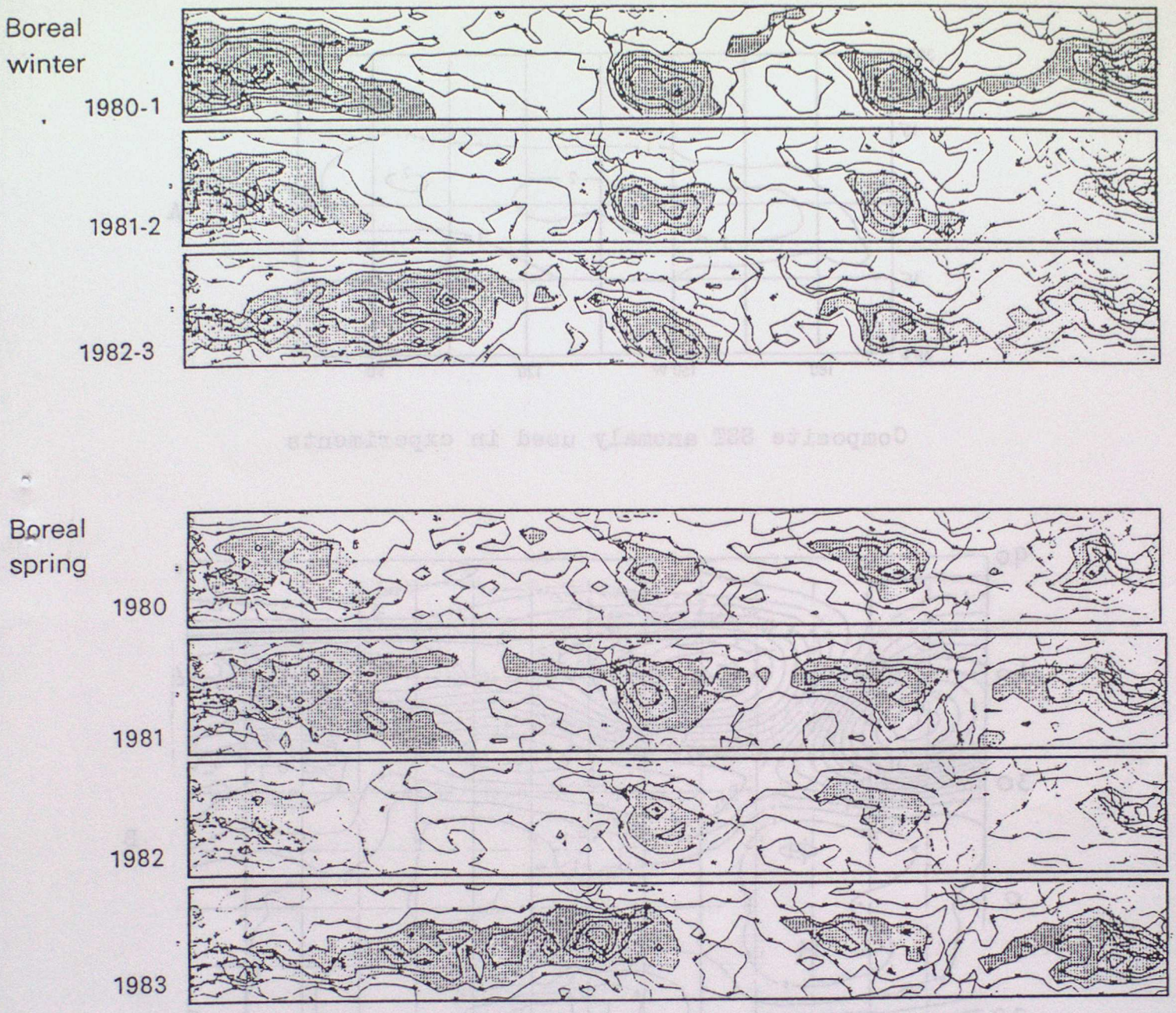

Figure 5.18. From Newman (1984).

Percentage cover of cloudtops with radiative temperatures less than 235° K. Contours drawn at 10% intervals. Areas of ⩾30% cloud cover are shaded.

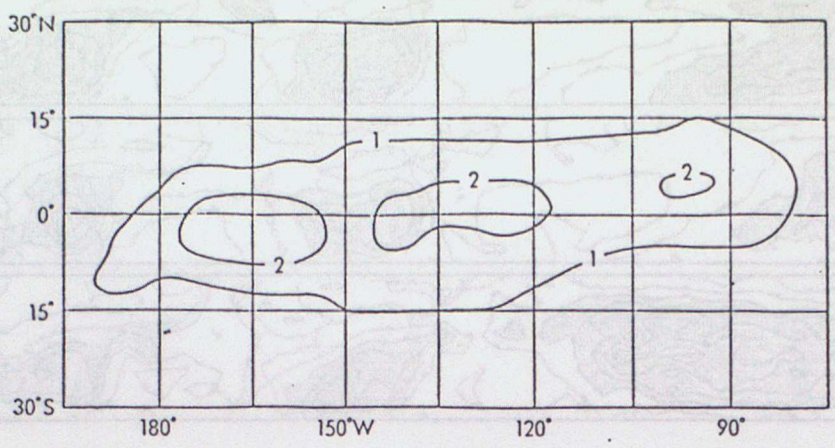

A

Composite SST anomaly used in experiments

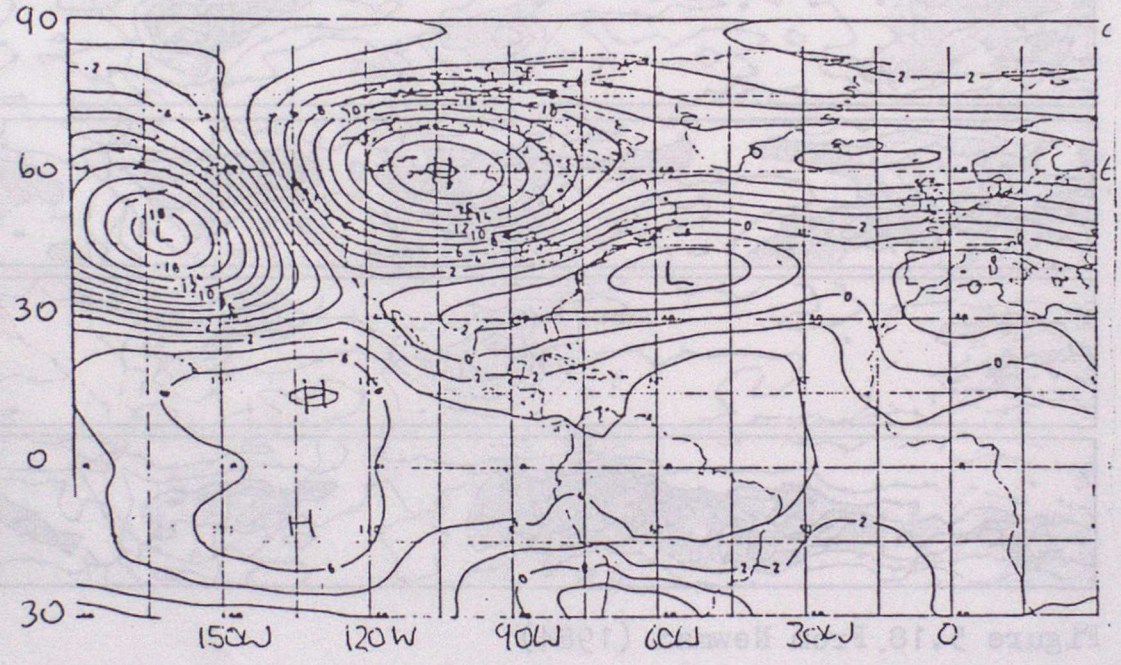

B

Anomalous 200mb height(dm) for
above composite SST anomaly

Figure 5.19. After Palmer (1985)

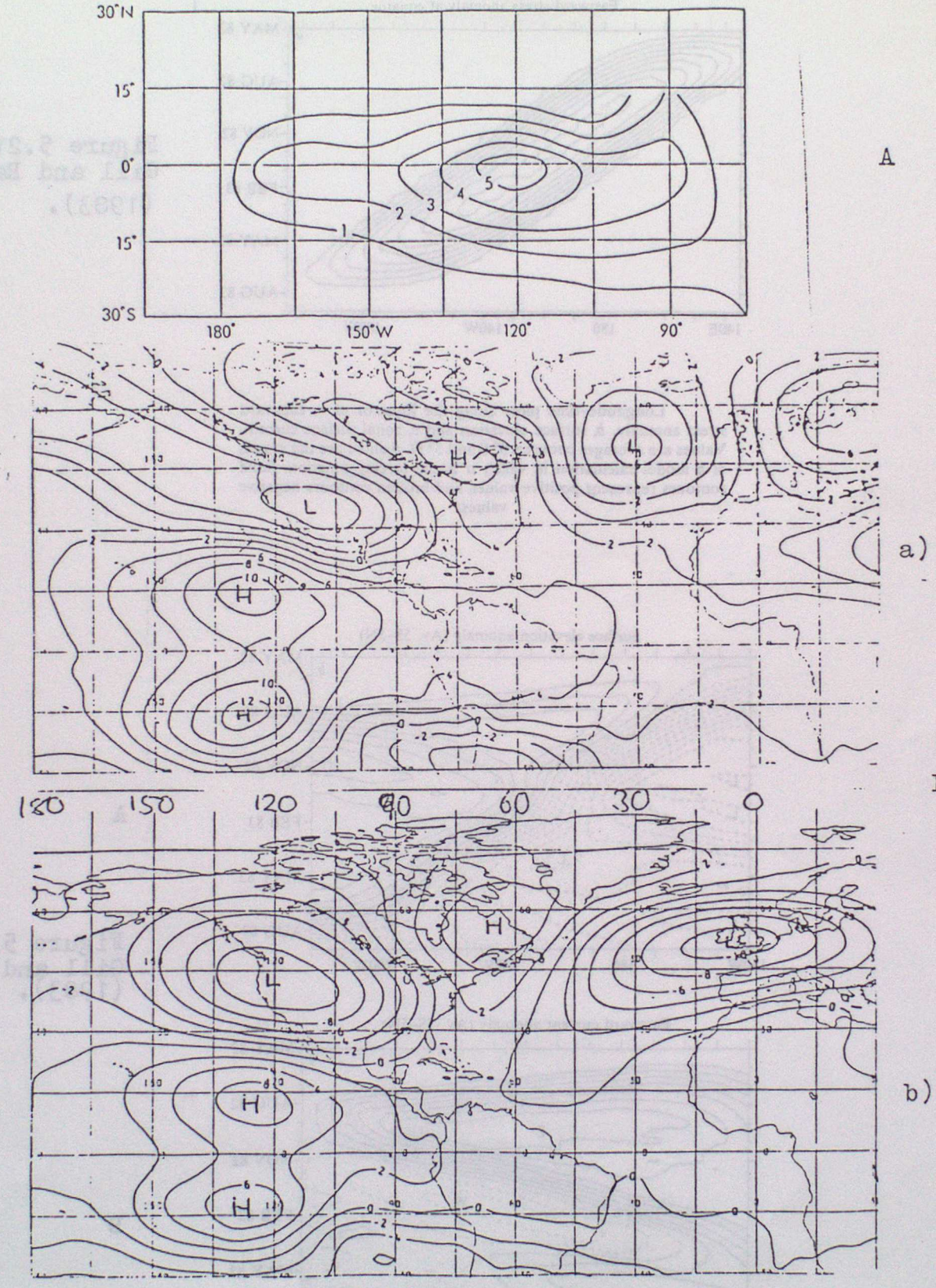

A: "El Nino" SST anomaly

B: Anomalous 200mb height (dm) when SST anomaly in A is applied a) with envelope orography b) with standard orography.

Figure 5.20. After Palmer (1985)

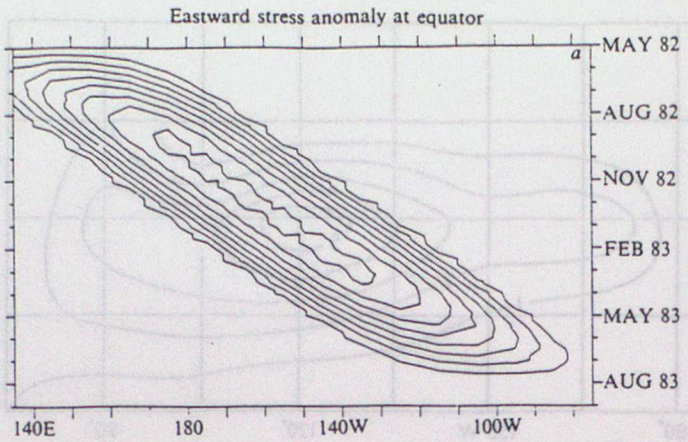

Figure 5.21, From Gill and Rasmusson (1983).

Longitude–time plots along the Equator of *a*, eastward stress anomaly, *b*, surface elevation and *c*, zonal surface current. Values are averages between 5° S and 5° N. *b* and *c* are the results of a model calculation in which *a* is the forcing function. Solid contours represent positive values and broken contours negative values.

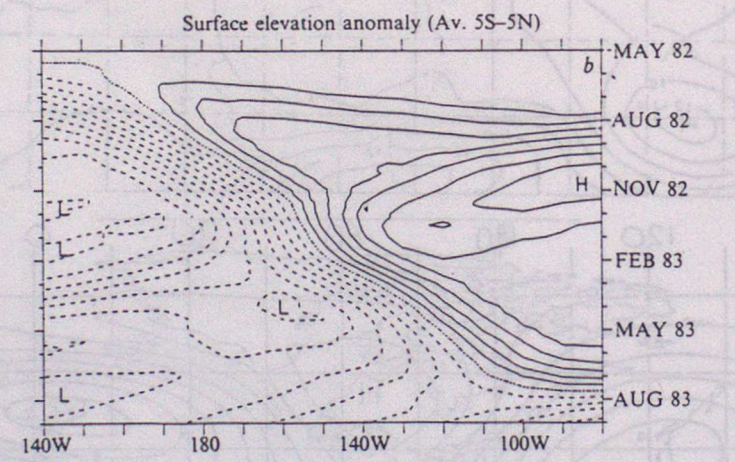

A

Figure 5.22. From Gill and Rasmusso (1983).

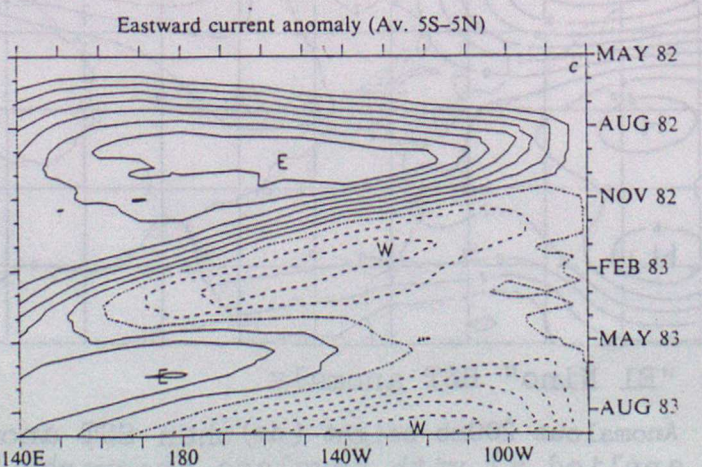

B

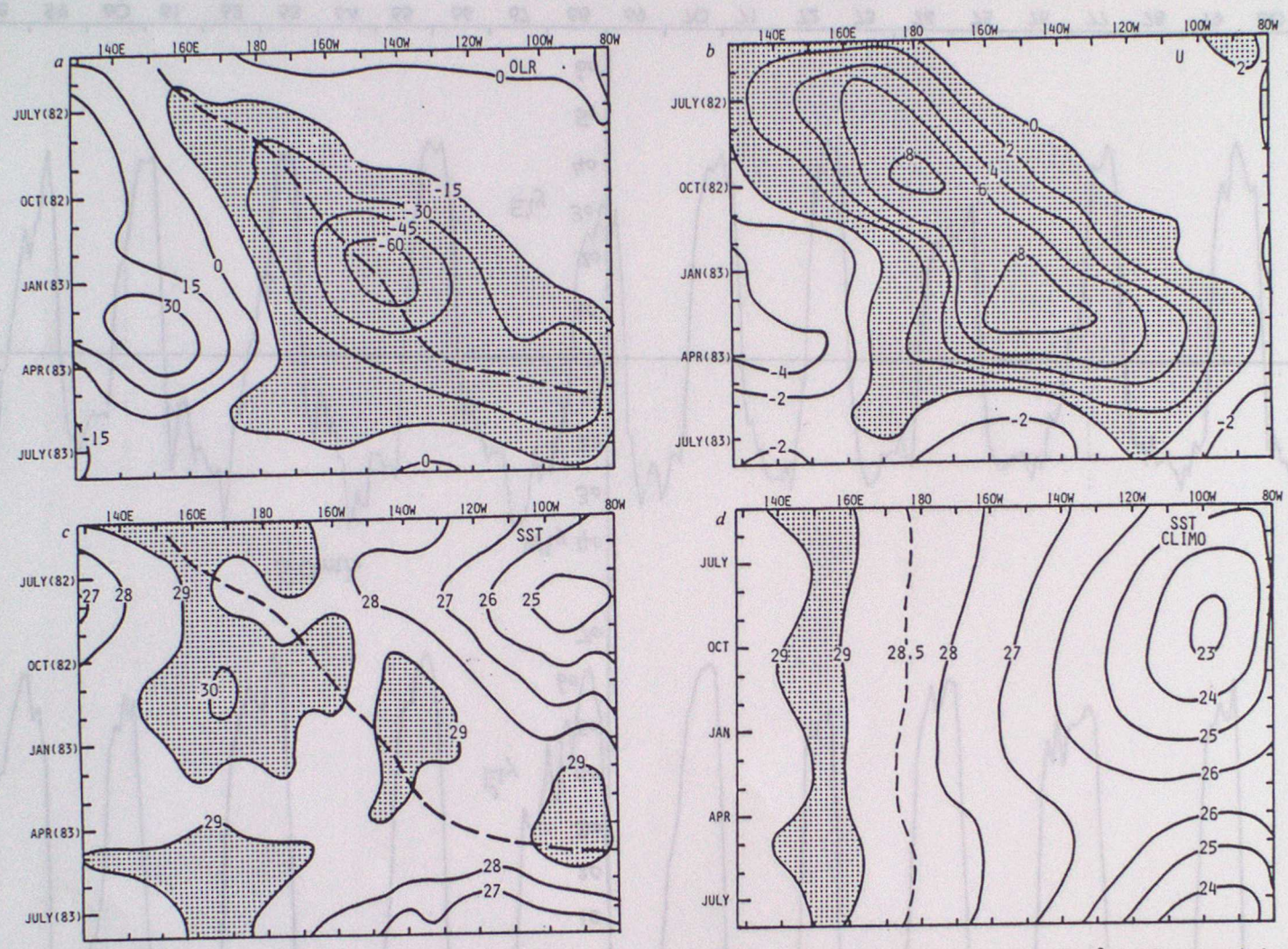

Longitude–time plots along the Equator of monthly mean values of *a*, OLR anomaly during 1982–83 in Wm^{-2}. *b*, Westerly wind anomaly (5° S–5° N) during 1982–83 in ms^{-1}. *c*, SST (4° S–4° N) during 1982–83. *d*, SST climatological mean values (from ref. 33, slightly smoothed). The dashed line in *a*, *c* follows the peak OLR anomaly.

Figure 5.23. From Gill and Rasmusson (1983)

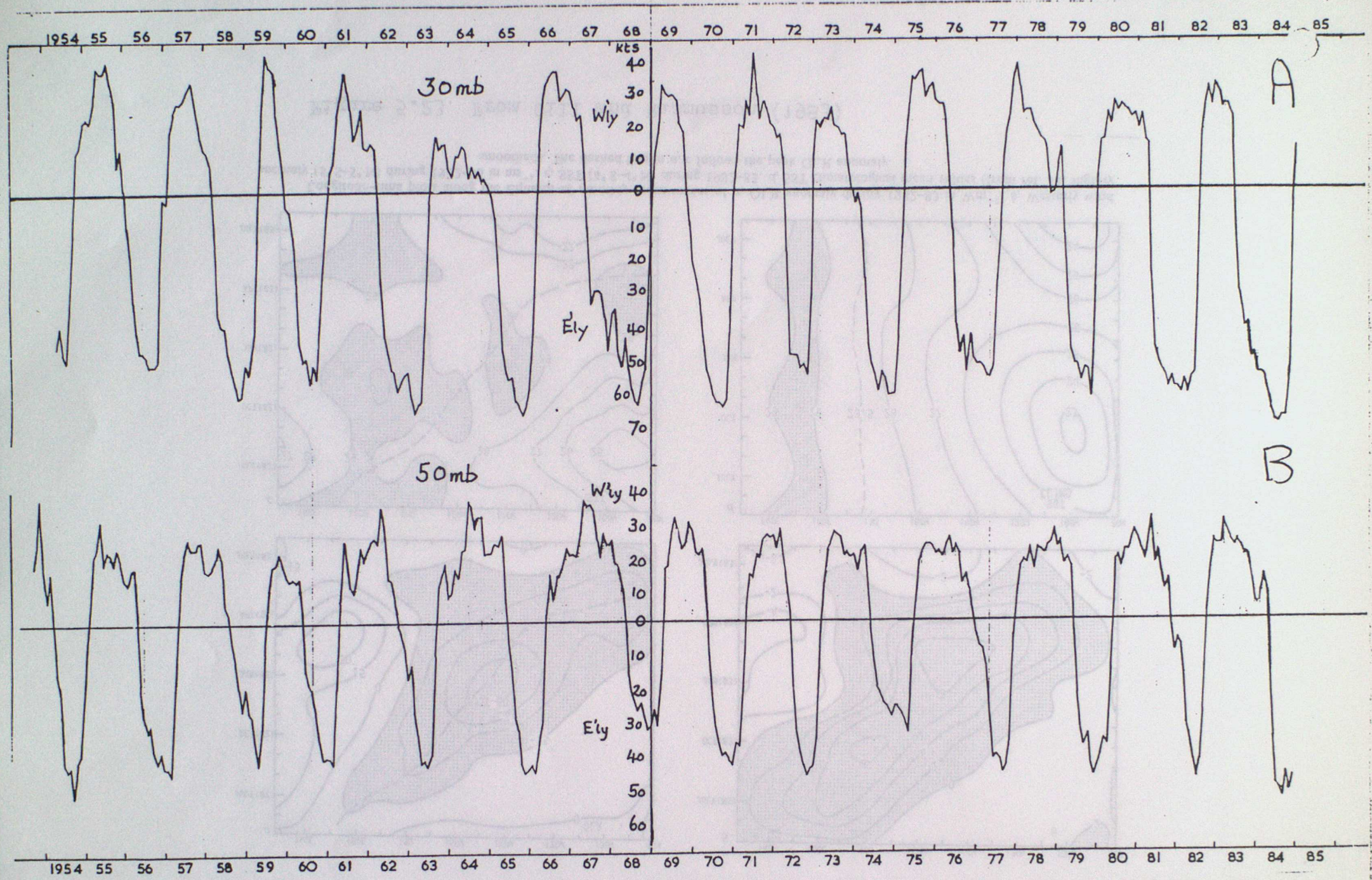

Monthly mean zonal wind components at 50 & 30 mb for Canton Island (2°46'S 171°43'W) from Oct 1953 – Aug 1967 & for Gan (00°41'S 73°09'E) from Sept 1967

(1°22'N 103°59'W) from Jul 1981

Figure 5.24

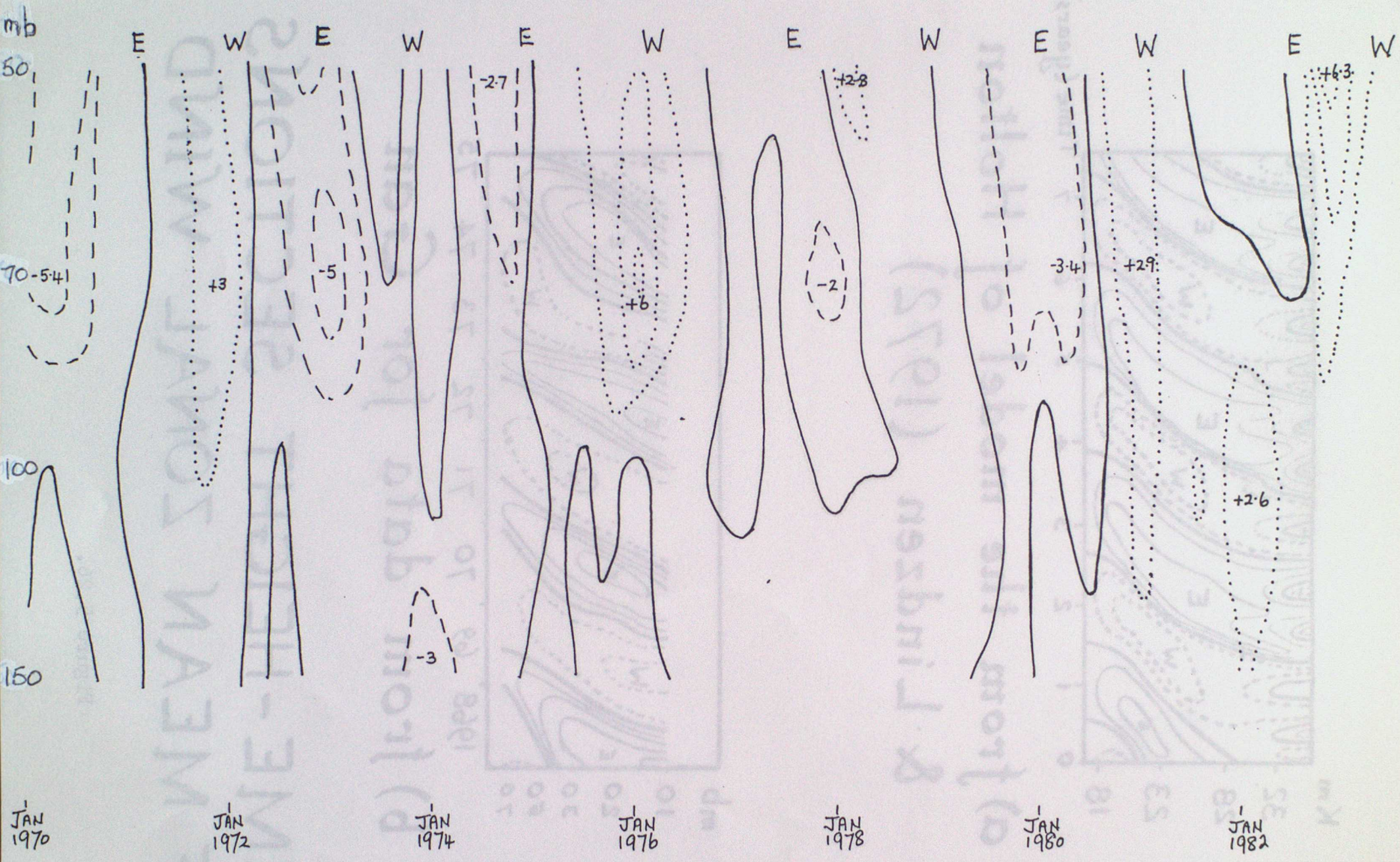

Figure 5.25. Temperature anomalies (wrt. 1971-80) over Singapore.
Isotherms at 2°C intervals

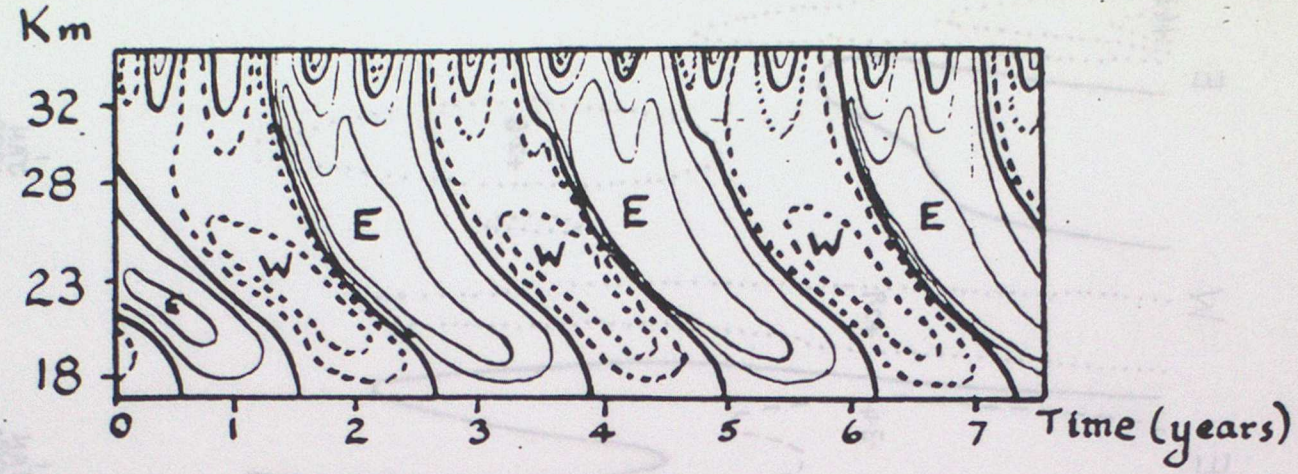

a) from the model of Holton & Lindzen (1972)

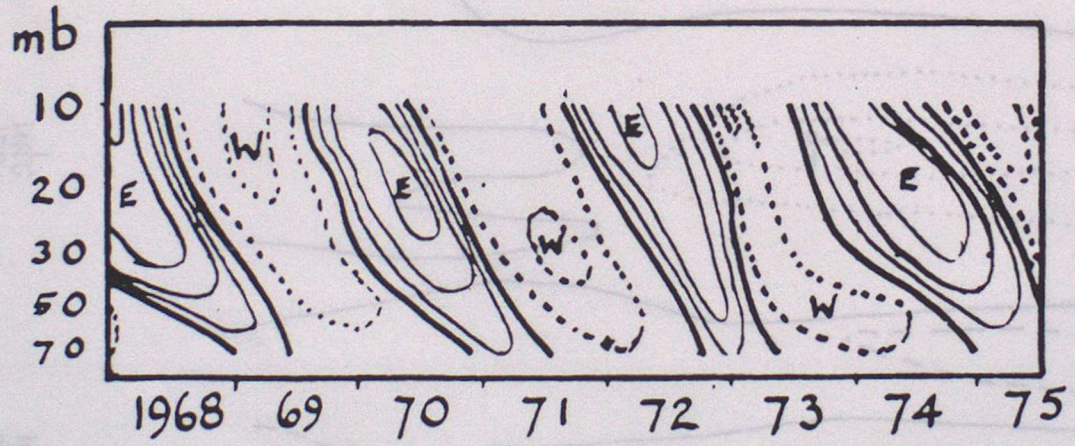

b) from data for Gan

TIME-HEIGHT SECTIONS OF MEAN ZONAL WIND

Figure 5.26.

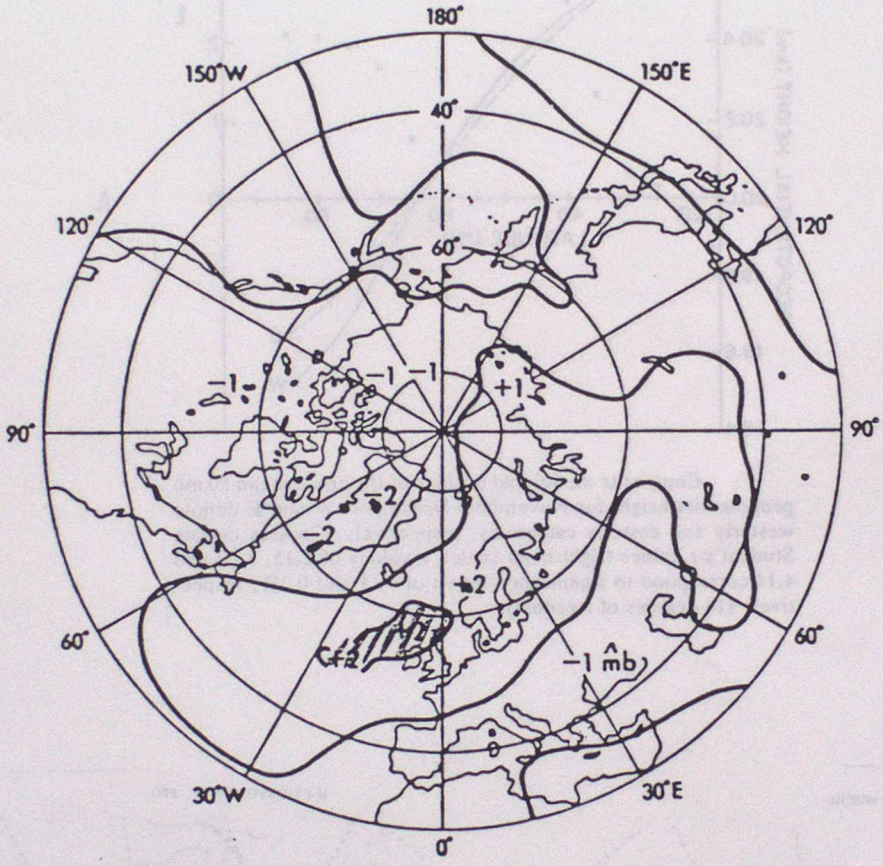

Surface pressure anomaly from 1951—70 average, July.
After Ebdon (1975).
Mean of eight Julys with westerly phase of QBO at 30 mb.

Figure 5.27.

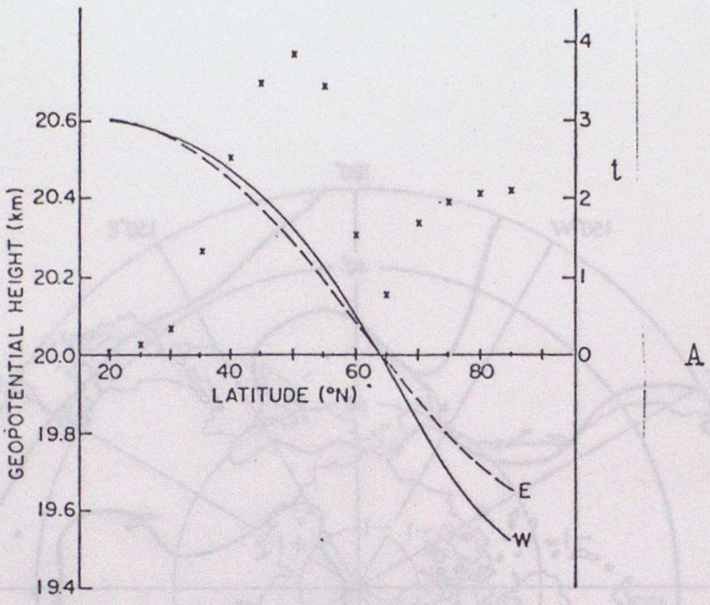

Composite meridional profiles of the zonal mean 50 mb geopotential height for November–December. W and E denote westerly and easterly categories, respectively. Crosses denote Student's t values (right hand scale). t values of 2.15, 3.00 and 4.14 correspond to significance levels of 5, 1 and 0.1%, respectively (14 degrees of freedom).

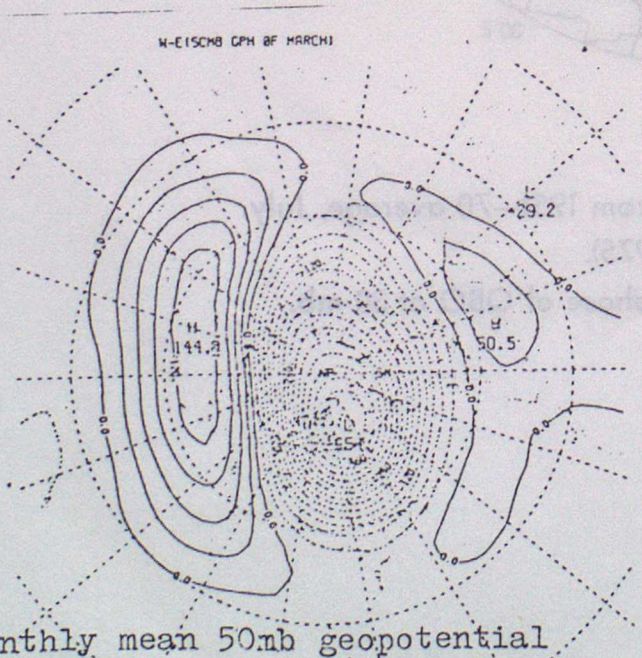

Monthly mean 50mb geopotential height difference (westerly minus easterly category) for Nov to Mar (9pm)

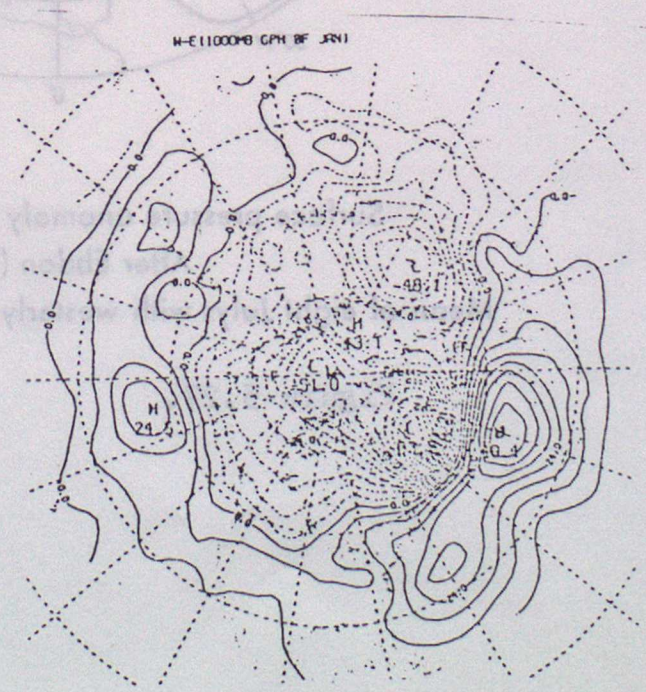

January mean 1000 mb geopotential height difference (westerly category minus easterly category). Units: geopotential meters.

Figure 5.28. From Holton and Tan (1980)